SUPPORTING INFORMATION – APPENDICES

Appendix S1 – Bandwidth selection for hypervolume calculation

The calculation of hypervolumes requires choosing a kernel bandwidth and quantile threshold that allow avoiding disjunctions, or 'holes'. Briefly, the calculation of a hypervolume for a set of points involves the sum of axis-aligned density kernels estimated for each point, in each dimension (see Blonder *et al.* 2014 for full description of the method); for small kernel bandwidths, or large threshold quantiles, the density kernels will include fewer of the adjacent points leading to a small hypervolume, with points appearing disjunct from the others (Blonder *et al.* 2014). Therefore, a large enough bandwidth (or small enough quantile threshold) must be chosen to avoid disjunctions. Since the choice of bandwidth will affect hypervolume size, we chose the same bandwidth to calculate all hypervolumes for a given component (raw and relative plant functional group, PFG, abundances or CWM trait values), so that hypervolumes could be directly compared. As for the quantile threshold we kept it at 0% following Blonder *et al.* (2014).

Optimal bandwidths were obtained by first calculating all hypervolumes (within a set of components) using a "free bandwidth" option (see *R* scripts in Appendix S5). This option allows an optimisation of the bandwidth value in function of the *disjunct factor*.
Given a starting value of bandwidth, hypervolumes are calculated and their disjunct factor is checked. The disjunct factor is the ratio between the size of the calculated hypervolume and the size of a hypervolume constructed from the same data with disjunct data points (i.e. no overlapping kernels; in R package 'hypervolume' Blonder *et al.* 2014). Values > 0.9 indicate that the hypervolume has 'holes' and should be avoided by increasing the bandwidth value. When this occurs, the bandwidth value is increased by 0.05 and the hypervolumes are re-calculated. The disjunct factor of the new hypervolumes is checked and bandwidth is further increased, if necessary.

We ran this process for all hypervolumes in all sets of components, with starting bandwidth values of 0.1, which were increased in steps of 0.05, when necessary, until the disjunct factor was ≤ 0.9. The maximum bandwidth value obtained across communities (i.e. combinations of scenario, habitat-land-use and repetitions) was then used as the fixed bandwidth value to re-calculate all hypervolumes. This ensured that all hypervolumes of a set of components were built with the same bandwidth value and that this value guaranteed a disjunct factor ≤ 0.9. For a) the analysis of differences between 'stable' states, bandwidths were 0.4 raw PFG abundances and 0.1 for relative PFG abundances and trait values. For b) the analysis of temporal stability, bandwidths were 0.75 for raw PFG abundances and 0.1 for relative PFG abundances.

Bandwidth sensitivity analysis

We assessed the effect of changing bandwidths by running a sensitivity analysis on a habitat under two types of land-use management. Thicket and scrubland areas had very consistent results across our analysis and provided two opposite extremes when under a scenario of land-use intensification: when areas grazed at low intensity ('grazed areas 1') were intensified hypervolumes did not intersect, whereas mown areas (which did not suffer land-use changes) always intersected. For each case, we built 10 pre- and 10 post-perturbation hypervolumes for different bandwidths, ranging from 0.1 to 1.0, in steps of 0.5. This one done for both raw PFG abundances and CWM trait values.

As expected, larger in bandwidths resulted in larger overlaps. For intensified grazed areas, results were qualitatively stable (i.e. overlap = 0) across the range of bandwidths tested in the case of raw PFG abundances, and up to 0.55 in the case of trait values (see Fig. 1 in this Appendix). Whereas in mown areas, intersections (overlap > 0) were present across all bandwidth sizes, except for one repetition of the smallest bandwidth (note that values of overlap where very small for this bandwidth value; Fig. 1). This meant that in neither case did our optimal bandwidths significantly affect the probability of an intersection (tested using a Generalised Linear Model with a logit link function to estimate the effect of bandwidth and land-use type on the probability of intersection; neither had a significant effect, p-value > 0.05). Also, increases in overlap size due to a larger bandwidth do not influence our results qualitatively, since they occur across all scenarios and habitat-land-use combinations.

Figure 1 – Evolution of proportion of overlap in function of bandwidth size. We chose thickets and scrubland habitats to assess the effect of increasing bandwidths on the proportion of overlap between control and post-perturbation hypervolumes of a) raw PFG abundances and b) community weighted mean trait values. This was done under a scenario of land-use intensification (scenario 3) and for areas presently grazed at low intensities, 'grazed areas 1' (which become grazed at high intensities) and presently mown areas (that suffer no land-use changes). Zero overlaps indicate an absence of intersection. Each point is the mean overlap between 10 pairs of hypervolumes and standard errors are shown as error bars.

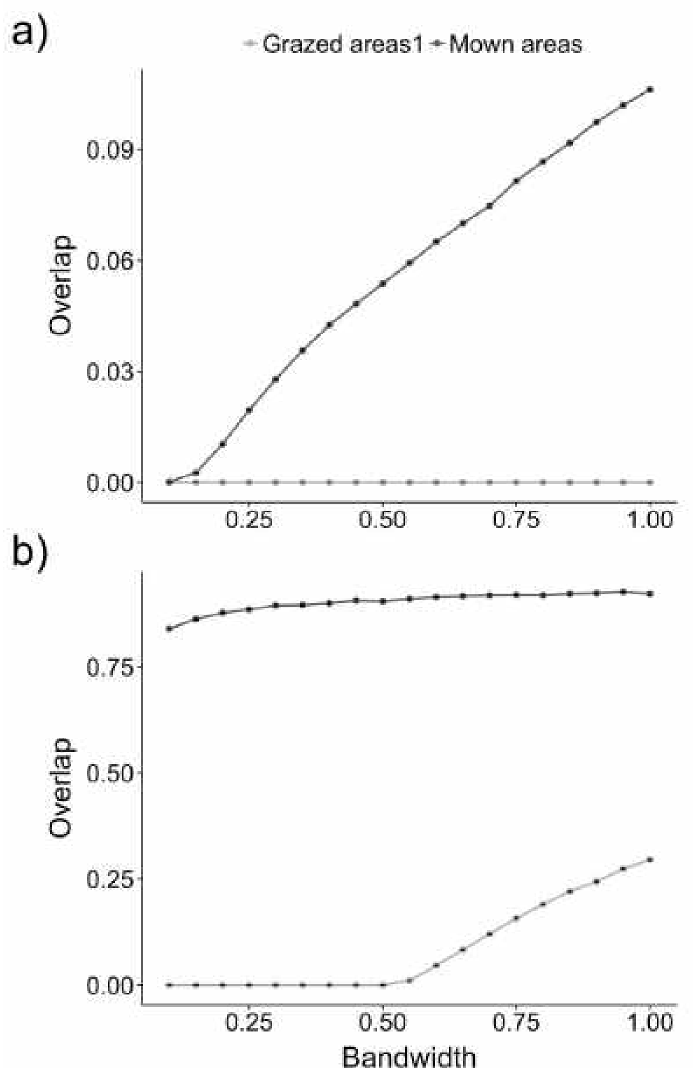

Appendix S2 – FATE-HD model description and simulation workflow

Model description

FATE-HD has been validated for the different plant communities present in the Ecrins National Park (ENP), situated in the southeast of France in the French Alps and covering an area of 178 400 ha. The ENP is characterized by mountainous to alpine ecosystems, its elevation ranging from 669m to 4102m a.s.l. Although large areas of the park are managed and used for different activities (around 68% of the total area), the park is a very diverse area with c. 2000 plant species. Grazing is the most important economic activity (occupying 48% of the total area), followed by forestry (10.5%) and agriculture (9.8%) (Esterni *et al.* 2006). Vegetation states are mostly maintained by abiotic conditions or land-use activities and can thus be expected to shift under climate and land use changes.

FATE-HD currently simulates 24 plant functional groups (PFGs) and five different height strata (0-1.5m; 1.5-4m; 4-10m; 10-20m; taller than 20m). They are divided into 6 chamaephyte groups (only present in the first height stratum, except for one which reaches the second one), 10 herbaceous groups (mostly hemicryptophytes and only present in the first height stratum) and 8 phanerophyte groups (all reaching at least the third height stratum, 6 reaching the fourth stratum and two reaching the fifth). Population dynamics, dispersal and competition for light resources are all explicitly included in the model for each PFG, being simulated across time and space. Population dynamics partially depend on habitat suitability, which is calculated from bioclimatic variables (Thuiller *et al.* 2009) and includes a stochastic component in order to simulate yearly oscillations of habitat quality. Climate changes, when introduced, affect habitat suitability by changing bioclimatic variables used to calculate it. Dispersal of PFGs is modelled for both long and short distances, which depend on the PFG in question. Competition for light resources is also modelled according to PFG type and stratum, as both differ in relation to their shade tolerance. The amount of shade is calculated per cell in function of the abundance of PFGs abundances per stratum. Disturbances are included in the model under two forms: grazing and mowing. Both grazing and mowing affect vegetation once a year, and grazing has three levels of intensity, low (1), medium (2) and high (3). They affect juvenile and mature plants abundances differently, depending on PFG responses to these disturbances and on an annual basis (see Boulangeat *et al.* 2014b for more information).

Land-use and climate changes

Climate changes were simulated according to IPCC previsions of the A1B scenario for years 2020, 2050 and 2080 and fed into future habitat suitability (HS) maps. These maps were then interpolated between time steps 2020, 2050 and 2080 to obtain a more gradual change at every 15 years for 90 years and later fed into FATE-HD simulations (for further details on construction of climate change maps see Boulangeat *et al.* 2014a).

Land-use changes followed one of three types: continuation of present management practices (business-as-usual), abandonment of all grazing and mowing activities and intensification of grazing in already grazed areas (to high intensity) with creation of new grazed and mown areas (see Boulangeat *et al.* 2014a for LU scenario justification).

Community/habitat types

Stability analysis fell unto communities, which were defined per habitat type following the present DELPHINE habitat classification of the ENP (Esterni *et al.* 2006). According to the DELPHINE classification there are 13 broad habitat categories present in the Ecrins (Table 1 in this Appendix). Non-colonized rocky habitats and rocky habitats in colonization were grouped due to their similarity. Habitats where no PFGs are present (glaciers, eternal snows and lakes), very specific habitats that FATE-HD cannot reproduce (ravines and wetlands) and highly artificial areas were excluded from the analysis (Table 1 in this Appendix). Habitat areas were then subset according to land-use type: non-disturbed areas, grazed areas of three intensities, mown areas and future grazed, mown and non-disturbed areas in the LU intensification scenarios.

Simulation workflow

Simulations started with an initialisation phase, ran over 1650 years, to achieve the current vegetation state of the ENP. It started with the seeding of all PFGs across the whole landscape for 300 years every year, followed by 300 years without any sort of LU management. Past deforestation was then simulated by cutting all PFGs in the second stratum or above (taller than 1.5m) from areas that are currently managed (years 600 and 800). Current management practices (grazing, with three levels of intensity and mowing) were only implemented afterwards (year 801) and the initialisation simulations were ran until year 1650.

Using outputs from the last initialisation year (1650), we simulated 6 scenarios of LU and, or, CC changes. Land-use changes were the abandonment of all grazing and mowing activities (scenario 2), business-as-usual (control scenario) and intensification of grazing and creation of new grazed and mown areas (scenario 3; Fig. 2) and then were repeated with presence of climate changes (scenarios 4-6 in Fig. 2). Land-use abandonment or intensification were applied 4 years after starting the simulation from initialisation outputs, whereas climate changes were applied from years 15 to 90, at every 15 years. Scenario outputs were saved on a yearly basis during 500 years.

An additional simulation of 100 years with no LU changes and no CC was run from the outputs from the last initialisation year (1650), to be used for proof-of-concept ('POC') comparisons to the control scenario.

All simulations were replicated 3 times and used corresponding 3 replicates from initialisation outputs as starting points.

Table 1 – Habitats used to define communities. Habitat classification followed the DELPHINE habitat classification of the Ecrins National Park (Esterni *et al.* 2006). Dashes indicate habitats removed from the analysis. Non-colonized and colonized rocky habitats were grouped under the “rocks” habitat type. FATE-HD output (yearly PFG abundances) was subset by habitat type and, within each habitat, by land-use type (grazed areas of intensities 1 to 3, mown areas, and non-disturbed areas and future grazed, mown and non-disturbed areas) resulting in 56 habitat-land-use combinations.

DELPHINE habitat code and designation	Details	Habitat
0. Glaciers and eternal snows		-
11. Lakes		-
14. Ravines	Water courses in deeply carved ravines	-
20. Wetlands	Swamps and stagnant water bodies	-
31. Non colonized rocks	10% or less vegetation cover	Rocks
36. Rocks in colonization	Scree and rocky areas with sparse vegetation	Rocks
40. Grasslands	Natural or artificial (includes cereal fields)	Grasslands
50. Lowlands	Alpine lowlands and lowlands with short woody vegetation (30-60cm) and some trees	Lowlands
60. Open habitats	Areas that can easily be invaded by shrubs and, or, trees; from hedged farmlands, to scrublands and grasslands and even scree and rocky cliffs	Open habitats
70. Semi-closed habitats	Generally mosaics of small woodlands and non-forested habitats that rapidly evolve to thickets or forests; composed	Woodland mosaics

	of tall or short woody species, with 40-60% closure	
81. Closed habitats	Impenetrable scrublands or thickets, that may have resulted from woody encroachment from past agricultural abandonment	Thickets/Scrubs
83. Forests	Dense forests with understory communities of grasses and shrubs	Forests
90. Artificial areas	Highly artificial environments, from roads and buildings, to gardens, vineyards and poplar/aspen production fields	-

Appendix S3 – Results obtained using relative PFG abundances

Another set of hypervolumes based on plant functional groups' (PFGs) abundances were built using relative abundances. These were calculated on a yearly basis and, as with other hypervolumes, the last 100 years of the scenarios of change were compared against the full 500 years of the control scenario. Proof-of-concept simulations were also compared against the control.

Hypervolume comparisons based on relative abundances mostly reflect changes in the evenness/dominance structure of communities. This means that communities must undergo quite large changes in their structure and, or, composition to result in new, post-perturbation, hypervolumes that do not intersect with their pre-perturbation counterparts. Results were in agreement with this, as intersections between hypervolumes were more frequent than those obtained with raw abundances, mean overlaps were generally larger, centroid distances were smaller and changes in hypervolume size (Δsize) were extremely small (see Figs. 1a, 2a and 3a in this Appendix). In accordance with results from raw abundances, climate change (CC) led to larger overall differences between pre- and post-perturbation communities. The combination of CC and land-use abandonment led to generally larger departures from initial community states, which was not always evident from raw PFG abundances. All of these three metrics were mostly affected by CC and land-use-changes (LUC) (Table 1 in this Appendix). Despite habitat-land-use combinations having a lower importance, some have shown to be more or less stable. For instance, low intensity grazing areas that suffered intensification showed consistently large departures from their pre-perturbed states across habitat types (see scenario 3 in 'grazed areas1' panel, Figs. 1b and 2b), whereas those that only suffered CC remained generally similar after perturbations (see scenario 5 in 'grazed areas1' panel, Figs. 1b and 2b). As with raw PFG abundances, mown areas (particularly in lowlands and thickets/scrublands) showed the largest changes in hypervolume size, mostly towards lower values (see ‘mown areas’ panel in Fig. 3b).

Finally, results for the analysis of the stability of overlap in time are in accordance with the patterns just observed. Like when comparing two states, tracking stability in time using relative abundances resulted in slower decreases in overlap in the communities under focus (Fig. 4 in this Appendix), than when using raw abundances. However, the patterns obtained were different (note that in Fig. 4 of this Appendix overlap was scaled using a square-root, but this does not change the qualitative interpretation of results). For instance, intensively grazed areas (‘grazed areas 3’) were the least stable communities in both habitat types (instead of mown areas, as seen with raw PFG abundances) and thickets and scrublands appear to be more stable than grasslands (with lower rates of decrease in overlap). This indicates that, although raw PFG abundances were quickly and strongly affected by changes in climate in both habitats and across land uses, thicket and scrubland community structure and composition were generally more stable, while grassland community structure and composition were stabilised under low intensity grazing, or no disturbances.

All in all, these results highlight that community structure remained more stable than PFG abundances in general, although being affected by both climate and land-use changes, the effects of which changed depending on the type of habitat and land-use management regime. Moreover, these results highlight the importance of taking care when choosing the community components that will constitute hypervolumes. As with choosing which taxonomic or functional diversity indices to use when studying perturbation effects, choosing to consider raw or relative abundances depends on the type of community changes one is interested in investigating.

Table 1 – Effects of climate change (CC), land-use changes (LUC), habitat-land-use combinations and management type on hypervolume metrics based on relative PFG abundances. Hypervolumes were compared using three metrics: proportion of overlap (overlap), distance between centroids and changes in hypervolume size (Δsize). Overlap was calculated as the ratio between the volume of intersection and the volume of the union. Size changes, or Δsize, were calculated as the difference between the size post-perturbation hypervolume size and the control hypervolume size. The response of each metric to climate changes, land-use changes and habitat-land-use combinations was modelled using analyses of variance (ANOVAs). To comply with linear model assumptions (normality and homoscedasticity of residuals), overlap values were modelled using a variant of the logit transformation, *log[(y+c)/(1-y+c)]* (where *c* is the absolute of the minimum non-zero observed value) and two extreme outliers were removed from the Δsize data. In all cases, the full model provided the best AICc score. Effects of main factors and interaction terms are shown in decreasing order of *F*-statistic. 'Df' stands for degrees of freedom, 'Sum Sq' for sums of squares, 'Mean Sq.' for mean squares and '*F* value' is the *F*-statistic.

		Df	Sum Sq	Mean Sq	*F* value	
Overlap						
$\sqrt{\text{Overlap}} \sim (\text{Habitat-land-use} + \text{CC} + \text{LUC})^{3\dagger\dagger}$	CC	1	27.57	27.57	623862.00	*
	LUC	2	22.14	11.07	250489.00	*
	CC:LUC	2	7.83	3.92	88605.00	*
	Habitat-land-use	55	15.73	0.29	6472.00	*

	CC:Habitat-land-use	55	11.61	0.21	4777.00	*
	LUC:Habitat-land-use	61	11.68	0.19	4331.00	*
	CC:LUC:Habitat-land-use	61	6.49	0.11	2407.00	*
	Residuals	476	0.02	0.00		
Centroid distances						
Centroid dist. ~ (Habitat - land - use + CC + LUC)^{3†}	CC	1	5.84	5.84	536916.00	*
	LUC	2	11.21	5.61	515694.00	*
	LUC:Habitat-land-use	61	8.82	0.15	13305.00	*
	CC:LUC	2	0.23	0.11	10422.00	*
	Habitat-land-use	55	6.08	0.11	10171.00	*
	CC:Habitat-land-use	55	1.56	0.03	2606.00	*
	CC:LUC:Habitat-land-use	61	0.86	0.01	1296.00	*
	Residuals	476	0.01	0.00		
Size changes						

$\Delta size \sim (Habitat - land - use + CC + LUC)^{3}$ †‡	CC	1	0.13	0.13	1196.30	*
	Habitat-land-use	55	1.04	0.02	169.26	*
	CC:Habitat-land-use	55	0.39	0.01	63.11	*
	CC:LUC:Habitat-land-use	61	0.23	0.00	33.01	*
	LUC:Habitat-land-use	61	0.22	0.00	32.90	*
	CC:LUC	2	0.00	0.00	16.25	*
	LUC	2	0.00	0.00	14.66	*
	Residuals	474	0.05	0.00		

[*] Significant at p-value < 0.01.

[†] Superscript "3" indicates the inclusion of all main factors and their two-way and three-way interactions in the model.

[‡] Two extreme outliers were removed from this model in order follow linear model assumptions.

Figure 1 – Proportion of overlap between hypervolumes based on relative PFG abundances. The a) observed mean proportion of overlap between control and post-perturbation hypervolumes are shown for each scenario, across all habitat types and grouped by disturbed areas (areas under present grazing or mowing regimes and areas that will become grazed on mown under scenarios of land-use intensification) and non-disturbed areas (all areas that are not currently grazed or mown and those that will remain so, under land-use intensification scenarios). Fitted overlap values in b) are shown for each scenario and habitat-land-use combination, and were obtained from analyses of variance detailed in Table 1 in this Appendix. Fitted values were back-transformed to be shown on the original scale. Standard errors of the observed means and of fitted values are shown as error bars. Comparisons between proof-of-concept (‘POC’) and control scenario hypervolumes are also shown.

1

a)

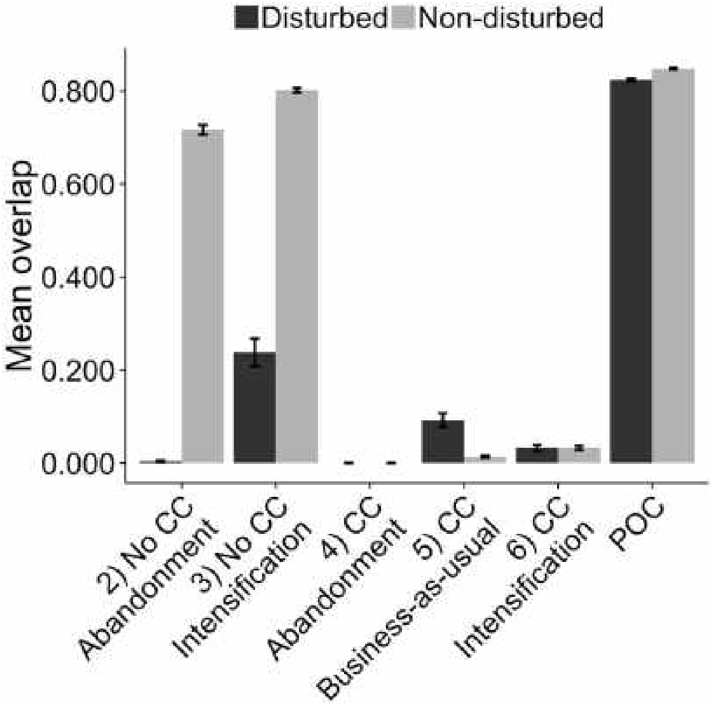
Disturbed
Non-disturbed
Mean overlap
0.800
0.600
0.400
0.200
0.000
2) No CC
Abandonment
3) No CC
Intensification
4) CC
Abandonment
5) CC
Business-as-usual
6) CC
Intensification
POC

b)

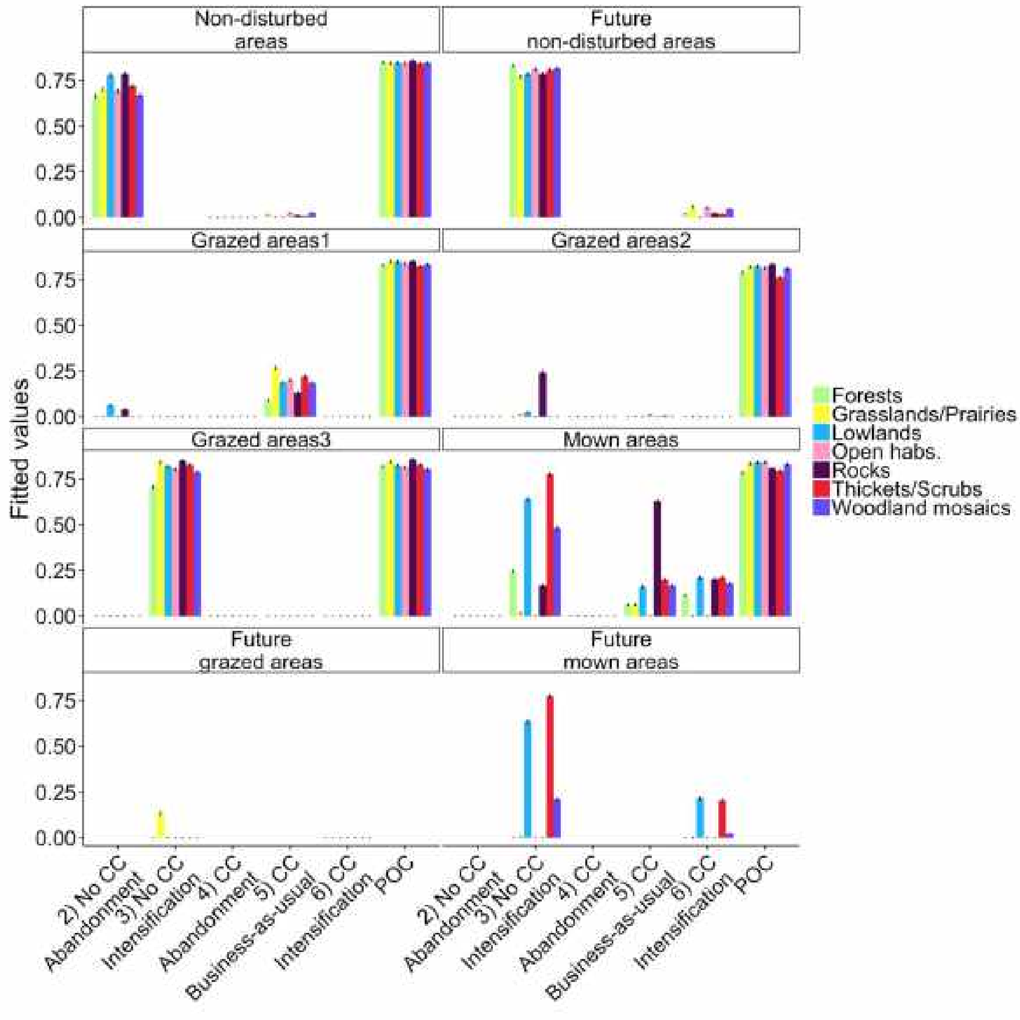
Non-disturbed
areas
Future
non-disturbed areas
Grazed areas1
Grazed areas2
Grazed areas3
Mown areas
Future
grazed areas
Future
mown areas
Fitted values
0.75
0.50
0.25
0.00
Forests
Grasslands/Prairies
Lowlands
Open habs.
Rocks
Thickets/Scrubs
Woodland mosaics
2) No CC
Abandonment
3) No CC
Intensification
4) CC
Abandonment
5) CC
Business-as-usual
6) CC
Intensification
POC

Figure 2 – Centroid distances between hypervolumes based on relative PFG abundances. The a) observed centroid distances between control and post-perturbation hypervolumes are shown for each scenario, across all habitat types and grouped by disturbed areas (areas under present grazing or mowing regimes and areas that will become grazed on mown under scenarios of land-use intensification) and non-disturbed areas (all areas that are not currently grazed or mown and those that will remain so, under land-use intensification scenarios). Fitted centroid distances in b) are shown for each scenario and habitat-land-use combination and were obtained from analyses of variance detailed in Table 1 in this Appendix. Standard errors of the observed means and of fitted values are shown as error bars. Comparisons between proof-of-concept ('POC') and control scenario hypervolumes are also shown.

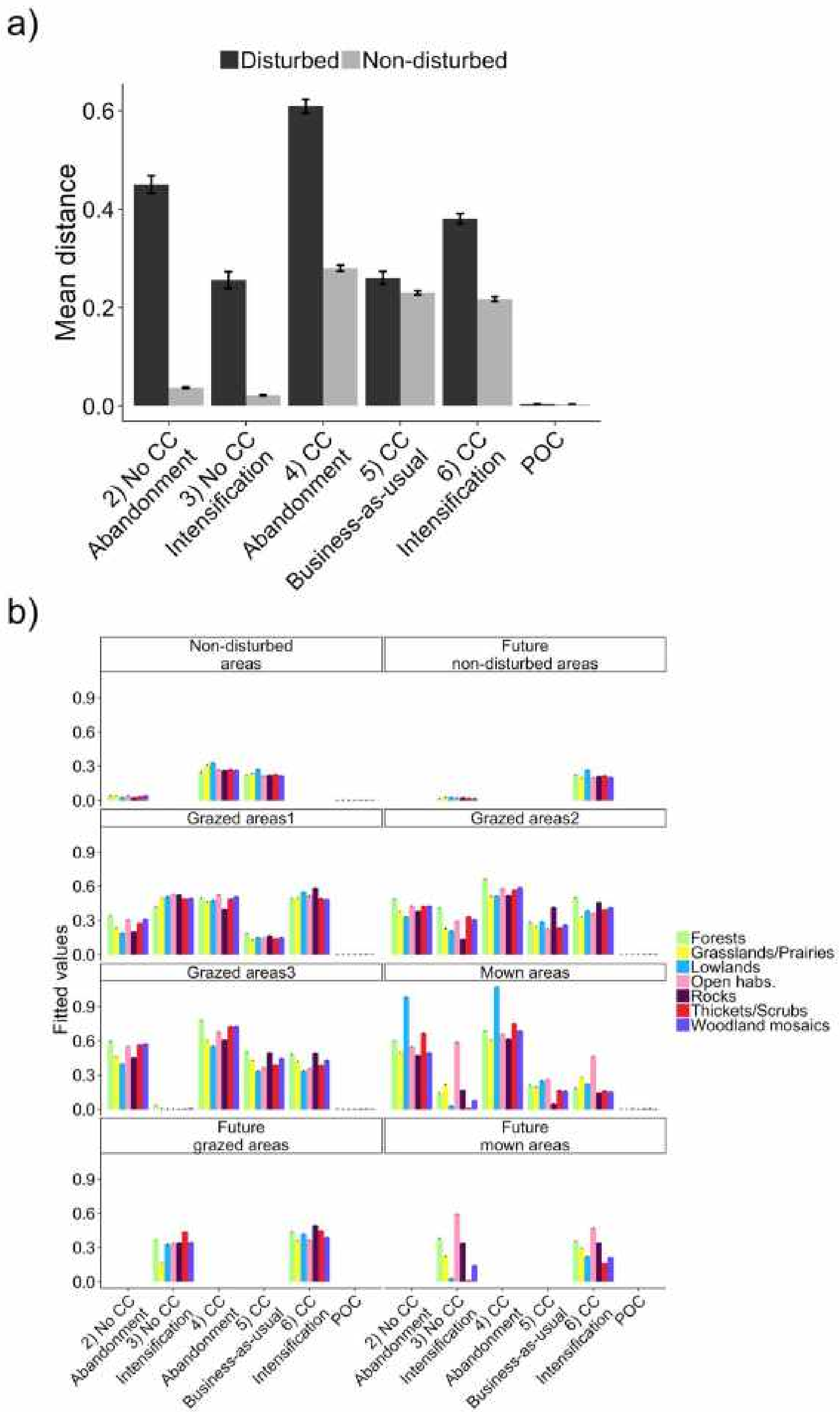

a)
Disturbed
Non-disturbed
Mean distance
0.6
0.4
0.2
0.0
2) No CC Abandonment
3) No CC Intensification
4) CC Abandonment
5) CC Business-as-usual
6) CC Intensification
POC
b)
Non-disturbed areas
Future non-disturbed areas
Grazed areas1
Grazed areas2
Grazed areas3
Mown areas
Future grazed areas
Future mown areas
Fitted values
0.9
0.6
0.3
0.0
Forests
Grasslands/Prairies
Lowlands
Open habs.
Rocks
Thickets/Scrubs
Woodland mosaics
2) No CC Abandonment
3) No CC Intensification
4) CC Abandonment
5) CC Business-as-usual
6) CC Intensification
POC

1

Figure 3 – Size differences between hypervolumes based on relative PFG abundances. The a) observed size changes (Δsize) from control to post-perturbation hypervolumes are shown for each scenario, across all habitat types and grouped by disturbed areas (areas under present grazing or mowing regimes and areas that will become grazed on mown under scenarios of land-use intensification) and non-disturbed areas (all areas that are not currently grazed or mown and those that will remain so, under land-use intensification scenarios). Negative Δsize values indicate that the post-perturbation hypervolume was smaller than its pre-perturbation counterpart, and vice-versa for positive Δsize values. Fitted Δsize in b) are shown for each scenario and habitat-land-use combination and were obtained from analyses of variance detailed in Table 1 in this Appendix. Standard errors of the observed means and of fitted values are shown as error bars. Comparisons between proof-of-concept ('POC') and control scenario hypervolumes are also shown.

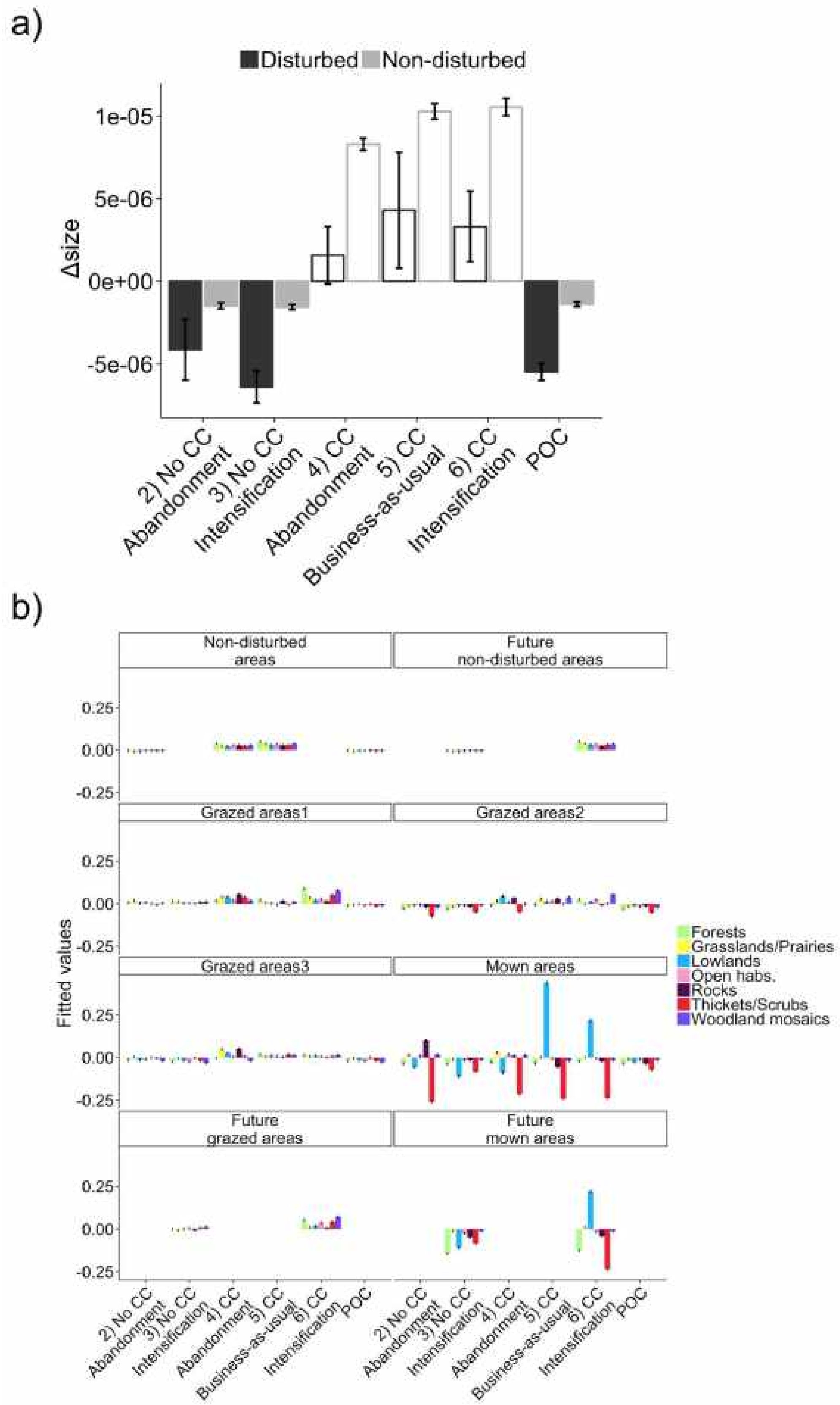
a)
Disturbed
Non-disturbed
Δsize
1e-05
5e-06
0e+00
-5e-06
2) No CC Abandonment
3) No CC Intensification
4) CC Abandonment
5) CC Business-as-usual
6) CC Intensification
POC
b)
Non-disturbed areas
Future non-disturbed areas
Grazed areas1
Grazed areas2
Grazed areas3
Mown areas
Future grazed areas
Future mown areas
Fitted values
0.25
0.00
-0.25
Forests
Grasslands/Prairies
Lowlands
Open habs.
Rocks
Thickets/Scrubs
Woodland mosaics

Figure 4 – Temporal stability measured by hypervolume overlap, based on relative PFG abundances. Temporal stability was analysed by modelling the temporal response of the square-root of proportion of overlap (overlap) under different habitat-land-use combinations, using generalised additive models (GAMs) with a Gaussian smoother fitted for each habitat-land-use combination. Each coloured point corresponds to the comparison between a hypervolume at a given time slice and the first hypervolume, with colours referring to land-use (the first year of each 15 year time slice is indicated in the x-axis). Dashed vertical lines indicate the start and end of simulated climate changes.

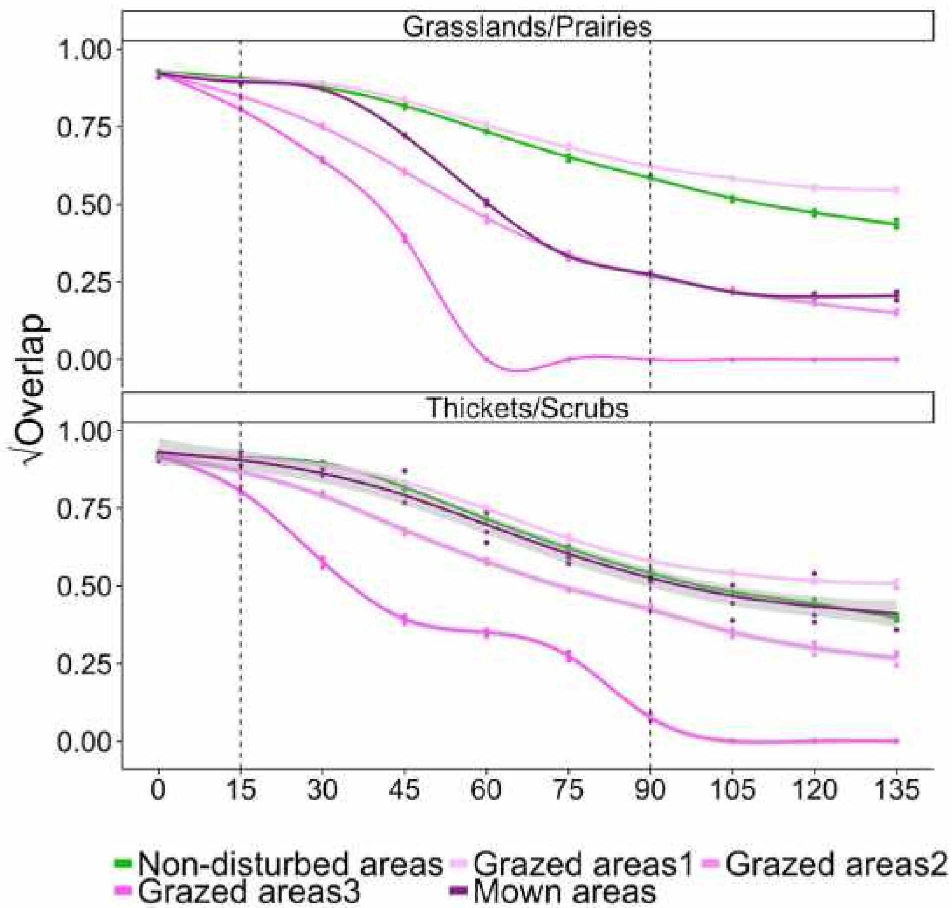

Appendix S4 – Choice and analysis of complementary metrics

In this appendix, we present the rational behind our selection of complementary metrics, as well as two additional functional diversity (FD) indices that were not presented in the main text, their statistical analyses and associated results. Results presented here are focused on these additional FD indices and we briefly discuss why they have not been included in the final manuscript.

Full set of complementary metrics

In the main manuscript we have presented 4 different complementary metrics that reflected changes in taxonomic (inverse Simpson concentration) and functional diversity (functional evenness and functional dispersion), and productivity (total plant functional group, PFG, abundances). However, in respect to FD, we have additionally calculated functional richness (FRic) and functional divergence (FDiv; Villéger *et al.* 2008) that were later excluded from the main text (see below).

Indices of taxonomic and functional diversity were chosen because they complemented the information given by hypervolumes built from raw PFG abundances or from community weighted mean (CWM) trait values. The inverse Simpson concentration reflects changes in PFG richness and evenness, which may not be reflected by hypervolumes based on raw abundances. Functional richness, evenness and divergence are three complementary, but independent, indices that reflect the occupied volume in the trait space, the regularity of abundances in trait space and how they diverge from each other (respectively; Villéger *et al.* 2008; Pavoine & Bonsall 2011; Tucker *et al.* 2016). Functional dispersion, is similar to FDiv, but accounts for the total volume occupied by PFGs in the trait space (Laliberté & Legendre 2010). These indices decompose the information accounted for in hypervolumes and offer a more detailed analysis of functional changes in the community. Lastly, productivity was included as a measure ecosystem functioning, following biodiversity and ecosystem functioning (BEF) studies.

Statistical analyses

Responses of diversity indices and productivity were fit with linear models using generalised least squares, with errors allowed to have an autoregressive structure at time lag-1 (the value of the correlation varying between each case). In parallel to what was done for hypervolume calculations, these analyses were done on the last 100 years of data; however, replicates were averaged. Time series of the control scenario (rather than proof-of-concept, 'POC', comparisons) were used as "no change" data that corresponded to no climate and no land-use changes. Because the experimental design was not balanced (i.e. disturbances like future grazing and mowing were only applied on scenarios 3 and 6) two sets of models were calculated. The first, 'set 1', aimed at analysing the effect of LUC, CC on habitats under current land-use practices (note that under scenarios of LU intensification – scenarios 3 and 6 – present grazing areas become grazed at high intensity). The second, 'set 2', aimed at analysing the effect of CC and habitat-land-use combinations on scenarios of LU intensification. For all models, future non-disturbed areas were grouped with non-disturbed areas, as they corresponded to the same treatment. Model selection followed AIC scores from more complex to simpler models. Model results were analysed in terms of the importance of main effects and interaction effects, and the differences between factor levels were analysed graphically.

No temporal autocorrelation was found when modelling the response of functional evenness (FEve) and functional dispersion (FDis) to CC and habitat-land-use combinations under the intensification scenario (set 2). Hence, their responses were analysed using analyses of variance (ANOVAs).

Results – FD indices

Since results concerning taxonomic diversity and productivity are presented in the main text, we focus here on results obtained for FD indices.

The importance of climate change (CC), land-use changes (LUC) and habitat-land-use combinations varied depending on the FD index (Table S3). For instance, habitat-land-use combinations had a comparatively strong effect on functional richness (FRic), but a weak effect on FEve and FDiv (set 1 models, Table S3). A graphical analysis of model fitted values showed that FRic and FDiv were the least responsive to the effects of predictor variables (Fig. S8a,d). Functional richness was equally low among scenarios for non-disturbed habitats and those under low and medium intensity grazing. Particular habitats, such as forests, thickets and scrublands and woodland mosaics showed higher FRic when under CC and high intensity grazing (Fig. S8a and S9a). This can be a reflection of increasing abundances of woody species, which benefit from climate warming in Alpine ecosystems (Tasser & Tappeiner 2002; Asner *et al.* 2004). In mown areas FRic was generally highest in lowlands under land-use intensification and, for other habitats, it seemed to also benefit from CC (Figs. S8a and S9a). As for FDiv, increases were mostly linked to land-use intensification and climate change (Figs. S8d and S9d). Contrarily to FRic, FDiv was generally lower in mown areas, but being increased under land-use intensification.

Functional evenness and FDis were more responsive to CC, LUC and habitat-land-use combinations (Figs. S8b,c and S9b,c). Their patterns were generally similar, with larger increases when land-use was abandoned and there was no CC. In some cases, however, FEve and FDis did not match. For instance, areas grazed at high intensity benefitted from CC in terms of FDis, but not so much in terms of FEve ('grazed areas3' in scenarios 5 and 6, Figs. S8b,c). In mown lowland habitats FDis also increased, whereas it decreased for FEve. These results indicate that in these communities functional variance increased as PFGs became less equally spread in trait space (Figs. S8b,c and S9b,c).

Selecting relevant functional diversity indices

As a rule of thumb, we propose choosing functional indices that, like hypervolume metrics, can reflect changes in a community's functional characteristics. Following Pavoine and Bonsall (2011) and Tucker *et al.* (2016), the indices we measured can be organised into three classes of measures of multivariate distances. Each class groups several indices together (Pavoine & Bonsall 2011; Tucker *et al.* 2016), but here we use only the most common ones.

- Richness. We use FRic (measured as the volume of the minimum convex hull occupied by all species, or in our case PFGs, in the trait space; Villéger *et al.* 2008) that indicates changes in the number of functionally unique identities in the community;
- Regularity (or evenness). We use FEve (Villéger *et al.* 2008) that indicates changes in the regularity of the distribution of species and their abundances in the functional trait space, and can be related to the variance in functional distances among PFGs (low variance = high regularity);
- Divergence. We use both FDis and FDiv that indicate changes in the mean abundance-weighted distances of species in functional space to the centroid of the functional space occupied by the community (which is also abundance-weighted for FDis, but not for FDiv; Villéger *et al.* 2008; Laliberté & Legendre 2010; Mouillot *et al.* 2013), thus providing a measure of the average functional distances between PFGs (Pavoine & Bonsall 2009; Laliberté & Legendre 2010; Pavoine & Bonsall 2011).

In our case, measures of FRic and FDiv had very similar results across scenarios of CC and LUC. Since FRic does not take PFG abundances into account, unless habitats gain or loose functionally distinct PFGs, FRic is expected to remain stable. Similarly, because in FDiv the functional centroid solely based on the PFGs at the vertices of the occupied functional space and is not abundance-weighted (functionally extreme PFGs; Villéger *et al.* 2008), FDiv values will remain fairly constant if changes in PFG abundances do not occur at the extremes of the functional trait space occupied by the community. Thus, FRic and FDiv are more affected by changes occurring at the extremes of the trait gradients. Hence, in our case, FEve and FDis provided a finer indication of changes in the functional structure of a community than FRic and FDiv, respectively.

We nevertheless believe that calculating a full set of FD indices that are uncorrelated (like FRic, FEve and FDis, or FDiv) from which some can later be selected, is not of bad practise. Since these indices provide information on different aspects of FD, unless there are clear expectations or convictions regarding changes of a particular aspect, their analysis can only be of interest to the understanding of functional changes that might have occurred in a community.

Appendix S6 – Supplementary results and discussion

Supplementary results

We present here the results obtained with raw PFG abundances and community weighted mean (CWM) trait values hypervolumes in more detail, especially in relation to habitat-land-use combinations.

Hypervolume intersections and overlap

The overlap between pre- and post-perturbation hypervolumes was mostly affected by climate change (CC) and land-use changes (LUC) (Table S3); yet, results also varied between habitats. Overlaps between raw PFG abundances were uncommon across most habitat-land-use combinations subjected to scenarios of change. However, comparisons between trait hypervolumes showed that areas kept undisturbed from both LUC and CC (non-disturbed areas in scenario 2 and future non-disturbed areas in scenario 3) were predicted to remain functionally more similar to their control scenario counterparts, as well as areas grazed at high intensity that suffered no changes (‘grazed areas 3’ in scenario 3) and thickets under mowing regimes (Fig. S3b). Similar results were obtained for relative PFG abundance hypervolumes (see Appendix S3).

Distances between hypervolumes and changes in size

Habitat-land-use combinations also had a weaker effect on mean PFG abundances and trait values than CC and LUC (Table S3). Nevertheless, changes in mean trait values seemed to depend on habitat type in intensively managed areas (see between-habitat differences in ‘grazed areas3’, mown areas and future grazed and mown areas; Fig. S5b). Also, undisturbed rock and scree vegetation showed consistently larger functional changes than other undisturbed habitats, but changes in PFG abundances were not as large, comparatively (see purple bars in present and future 'non-disturbed' areas, Fig. S5).

Changes in the variance of PFG abundances and trait values, however, were more affected by habitat-land-use combinations (Table S3). Areas grazed at high intensities and mown areas showed larger Δsize values across several habitats and scenarios of CC and LUC (see 'grazed areas3' and mown and future mown areas panels Fig. S6).

Finally and in accordance with intersection results, the majority of unmanaged habitats seemed to suffer larger changes in mean PFG abundances than in CWM trait values, even when suffering no CC (see non-disturbed and future non-disturbed areas in scenarios 2 and 3, respectively, in comparison to POC; Fig.S5), but this did not result in large changes in variance (Fig. S6).

Supplementary discussion

Taxonomic and functional changes in non-disturbed rock and scrub vegetation

Unlike other undisturbed habitats, rock and scree vegetation showed larger functional changes (relatively to taxonomic deviations) than other habitats, even under no climate change (non-disturbed areas in scenario 2 and future non-disturbed areas in scenario 3, Figs. S3b and S5b). Rocky habitats can be found at relatively high elevations at the core of the Ecrins (Fig. S1), where environmental filtering is likely to lead to relatively low functional α-diversity (de Bello *et al.* 2013). Colonisations resulting from spill over effects could cause functional changes in these communities, even if not causing large changes on overall taxonomic and functional α-diversity (Figs. S7a and S8b,c). Under climate change, rocky habitats have also shown larger changes in mean plant functional group (PFG) abundances and increases in PFG α-diversity, in opposition to other habitats (scenarios 4-6, Figs. S5a and S7). Although FATE-HD has a tendency to over-predict tree cover in rocky habitats

(Boulangeat *et al.* 2014b), our results agree with observations of range expansions of alpine species towards higher elevations, accompanied by range contractions of sub-nival and nival species (Pauli et al. 2007; Gottfried et al. 2012).

Potential applications in terms of ecosystem resilience

Our approach does not yet provide a parallel with the quantification of resilience in terms of rates of return to stability after perturbations – engineering resilience – or the magnitude of perturbation a community can withstand before shifting states – ecological resilience (sensu Holling 1996; Gunderson 2000). Instead, considering multiple community components links different facets of biodiversity and ecosystem stability, a key aspect of ecosystem resilience (Norberg 2004; Cadotte et al. 2012; Mori et al. 2013). Nevertheless, we can foresee how the framework we provide can be related with the two aspects of resilience defined by Holling (1996). Understanding if the overlap between hypervolumes depends on the magnitude of the applied perturbation can provide clues as to the amount of change at community can suffer before shifting to another state, indicating the width of the basin of attraction and the community's ecological resilience. On the other hand, the time it takes for hypervolumes to return to their original state after a perturbation can be related to engineering resilience. Also, time series of hypervolume metrics, such as hypervolume size, calculated in the vicinity of a state shift could be used to detect phenomena like critical slowing down and flickering (early warning signals; Scheffer *et al.* 2009; Dakos *et al.* 2012), which would be reflected in changes of statistical properties of the hypervolume metrics' time series. The limitations being that 1) very large and complete time series would be necessary to calculate enough hypervolumes and statistical analyses on their metrics, and 2) that early warning signals do not occur under several cases, such as systems under push-perturbations (non-gradual changes in external variables), or for systems with chaotic behaviour (Dakos *et al.* 2015; Sharma *et al.* 2015).

Importantly, our framework allows an analysis of ecosystem stability under different perspectives. Not only can it provide a measure of departures from equilibrium within a same basin of attraction (see Fig. 1e in the main text), but it can also be used to study alternative stable states (Fig. 1f) or shifts in the stable state *per se* after changes in the system's parameters (Fig. 1g; see also Beisner *et al.* 2003; Horan *et al.* 2011)

SUPPORTING INFORMATION – TABLES

Table S1 – Plant functional groups and their trait values. Trait values were averaged across species for continuous traits and the majority class was taken for ordinal traits (see further details in Boulangeat *et al.* (2012)). Life form classes are chamaephytes (C), herbaceous (H) and phanerophytes (P). We selected four traits, three reflecting the leaf-height-seed (LHS) plant ecology strategy by Westoby (1998) – average specific leaf area (SLA), log height, log seed mass – and one reflecting plant responses to grazing – palatability. Traits with an asterisk were log-transformed for all analysis to approach a normal distribution; however, in this table we present only the non-transformed values. SLA values for species of PFGs H10 and P8 obtained from (Kattge *et al.* 2011). Table partially adapted from Boulangeat *et al.* (2012).

PFG	**PFG description**	**Average SLA (mm^2/mg)**	**Height* (cm)**	**Seed mass* (mg)**	**Palatability (class)**
C1	Thermophilous chamaephytes with long dispersal distances	19.21	27	23.91	3
C2	Alpine and subalpine chamaephyte species	18.02	13	0.38	3
C3	Chamaephytes with short dispersal distances	14.39	7	0.51	0
C4	Tall shrubs	16.83	209	192.99	2
C5	Dry climate mountainous to subalpine heath	8.28	76	75.01	0
C6	Wet climate mountainous to subalpine heath	13.40	18	39.50	2
H1	Alpine species (with no shade tolerance and with short dispersal distances)	17.22	17	0.86	3

H2	Mountainous species tolerant of nitrophilous soils and with long dispersal distances	22.11	42	4.04	3
H3	Mountainous to lowland species found in wet niches and with long dispersal distances	24.43	50	2.37	3
H4	Undergrowth and shadow-tolerant species, but that do not tolerate full light	29.76	76	0.36	0
H5	Mountainous to subalpine species, tolerant of dry soils and with short dispersal distances	20.71	40	1.94	3
H6	Tall plants typical of 'mégaphorbiaies', which can form undergrowth	28.21	73	2.31	3
H7	Species found in rocky habitats and undergrowth at all elevations	19.25	19	0.40	0
H8	Subalpine to alpine species not usually grazed and with short dispersal distances	23.11	19	0.89	0
H9	Short subalpine to alpine species with long dispersal distances	21.09	19	0.38	3
H10	Mountainous species, shade tolerant and with long dispersal distances	21.14	100	6.20	3
P1	Thermophilous pioneer trees (deciduous trees and pines)	12.03	1175	177.93	2
P2	Small deciduous pioneer trees (e.g. colonising riversides)	17.17	750	0.13	2
P3	Tall forest edge trees	15.30	1667	86.41	2

P4	Tall pioneer (larch)	10.06	2500	6.82	0
P5	Wet climate late succession trees	11.86	2500	114.06	2
P6	Dry climate intermediate succession trees	19.24	1650	6.10	2
P7	Small forest edge trees	15.65	600	78.27	2
P8	Small pioneer found in cold climates (white birch)	14.60	800	0.17	2

Table S2 – Effects of climate change (CC), land-use changes (LUC), habitat-land-use combinations and management type on hypervolume metrics. Hypervolumes were compared using three metrics: proportion of overlap (overlap), distance between centroids and changes in hypervolume size (Δsize). Overlap was calculated as the ratio between the volume of intersection and the volume of the union. Δsize were calculated as the difference between the size post-perturbation hypervolume size and the control hypervolume size, after scaling all sizes in respect to the larges hypervolume obtained for a set of components. The response of each metric to climate changes, land-use changes and habitat-land-use combinations was modelled using analyses of variance (ANOVAs). To comply with linear models' assumptions (normality and homoscedasticity of residuals), we used a square-root transformation on overlap values (for both PFG and trait hypervolumes) and removed three extreme outliers from the trait hypervolumes Δsize data. In all cases, the full model provided the best AICc score. Effects of main factors and interaction terms are shown in decreasing order of *F*-statistic. 'Df' stands for degrees of freedom, 'Sum Sq' for sums of squares, 'Mean Sq.' for mean squares and '*F* value' is the *F*-statistic.

		Df	**Sum Sq**	**Mean Sq**	***F* value**	
PFG hypervolumes overlap						
$\sqrt{\textbf{Overlap}} \sim (\textbf{Habitat-land-use} + \textbf{CC} + \textbf{LUC})^{3\dagger}$	LUC	2	18.79	9.39	42945.73	*
	CC:LUC	2	18.72	9.36	42793.66	*
	CC	1	9.11	9.11	41649.23	*
	CC:Habitat-land-use	55	2.51	0.05	208.32	*

	Habitat-land-use	55	2.50	0.05	207.73	*
	CC:LUC:Habitat-land-use	61	0.41	0.01	30.58	*
	LUC:Habitat-land-use	61	0.38	0.01	28.76	*
	Residuals	476	0.10	0.00		
PFG hypervolumes centroid distances						
Centroid dist. ~ (Habitat - land - use + CC + LUC)^{3†}	LUC	2	3721.00	1860.50	130243.50	*
	CC	1	517.00	516.90	36184.44	*
	CC:LUC	2	316.00	157.90	11050.73	*
	LUC:Habitat-land-use	61	776.00	12.70	890.09	*
	Habitat-land-use	55	547.00	10.00	696.72	*
	CC:Habitat-land-use	55	200.00	3.60	254.09	*
	CC:LUC:Habitat-land-use	61	70.00	1.10	79.91	*
	Residuals	476	7.00	0.00		
PFG hypervolumes size change						

$\Delta size \sim (Habitat - land - use + CC + LUC)^{3\dagger}$	LUC	2	1.34	0.67	901.17	*
	Habitat-land-use	55	17.00	0.31	414.59	*
	LUC:Habitat-land-use	61	4.71	0.08	103.52	*
	CC	1	0.03	0.03	37.54	*
	CC:LUC	2	0.03	0.02	20.73	*
	CC:Habitat-land-use	55	0.79	0.01	19.24	*
	CC:LUC:Habitat-land-use	61	0.67	0.01	14.76	*
	Residuals	476	0.36	0.00		
Trait hypervolumes overlap						
$\sqrt{Overlap} \sim (Habitat - land - use + CC + LUC)^{3\dagger}$	CC	1	21.75	21.75	169764.50	*
	LUC	2	18.46	9.23	72055.50	*
	CC:LUC	2	16.93	8.46	66078.50	*
	Habitat-land-use	55	11.76	0.21	1668.80	*
	CC:Habitat-land-use	55	9.36	0.17	1328.60	*

	LUC:Habitat-land-use	61	5.33	0.09	682.40	*
	CC:LUC:Habitat-land-use	61	4.61	0.08	589.50	*
	Residuals	476	0.06	0.00		
Trait hypervolumes centroid distances						
Centroid dist. ~ (Habitat - land - use + CC + LUC)^{3}†	LUC	2	155.14	77.57	290381.00	*
	CC	1	44.21	44.21	165496.00	*
	CC:LUC	2	19.44	9.72	36385.00	*
	Habitat-land-use	55	213.38	3.88	14523.00	*
	LUC:Habitat-land-use	61	120.54	1.98	7397.00	*
	CC:Habitat-land-use	55	64.81	1.18	4411.00	*
	CC:LUC:Habitat-land-use	61	41.16	0.67	2526.00	*
	Residuals	476	0.13	0.00		
Trait hypervolumes size change						
Δsize ~ (Habitat - land - use + CC + LUC)^{3}†‡	CC	1	0.04	0.04	1799.07	*

	CC:LUC	2	0.01	0.01	244.74	*
	CC:Habitat-land-use	55	0.22	0.00	190.56	*
	LUC	2	0.01	0.00	125.60	*
	Habitat-land-use	55	0.12	0.00	103.51	*
	CC:LUC:Habitat-land-use	60	0.12	0.00	98.05	*
	LUC:Habitat-land-use	61	0.08	0.00	59.62	*
	Residuals	474	0.01	0.00		

[*]Significant at p-value < 0.01.

[†]Superscript “3” indicates the inclusion of all main factors and their two-way and three-way interactions in the model.

[‡]Three extreme outliers were removed from this model in order follow linear models’ assumptions.

Table S3 – Effects of climate change (CC), land-use changes (LUC), habitat-land-use combinations and management type on complementary metrics. Responses of taxonomic (PFG α-diversity) and functional diversity (FRic, FEve, FDis, FDiv), as well as productivity to effects of climate change, land-use change and habitat-land-use combinations were modelled fort he last 100 years of the scenario and control simulations. To account for temporal autoregressive structures models were separated in two sets to have a balanced design. Models in 'set 1' investigated the effects of CC and LUC on "current" habitat-land-use combinations and models in 'set 2' investigated the effects of CC and all habitat-land-use combinations on scenarios of LU intensification. Model selection was based on AIC scores. The response of each metric to climate changes, land-use changes and habitat-land-use combinations was modelled accounting for an autoregressive structure at time lag-1. Not temporal autocorrelations were found for set 2 models of FEve and FDis, which were modelled using analyses of variance (ANOVAs). Best models were selected on the basis of AIC scores. Effects of main factors and interaction terms are shown in decreasing order of *F*-statistic. 'Df' stands for degrees of freedom, 'Sum Sq' for sums of squares, 'Mean Sq.' for mean squares and '*F* value' is the *F*-statistic.

			Df	***F*-value**	
SET 1	**PFG α-diversity**				
	AlphaDiv ~ (Habitat-land-use + CC + LUC)^{3†}	(Intercept)	1.00	61.85	*
		CC	1.00	2.52	
		LUC	2.00	1.62	

		CC:LUC	2.00	0.87	
		Habitat-land-use	34.00	0.26	
		CC:Habitat-land-use	34.00	0.05	
		LUC:Habitat-land-use	68.00	0.04	
		CC:LUC:Habitat-land-use	68.00	0.01	
SET 2	**PFG α-diversity**				
	AlphaDiv ~ (Habitat-land-use + CC)^{2†}	(Intercept)	1.00	22.48	*
		Habitat-land-use	48.00	0.21	
		CC	1.00	0.09	
		CC:Habitat-land-use	48.00	0.02	
SET 1	**Trait α-diversity (FRic)**				
	FRic ~ (Habitat-land-use + CC + LUC)^{3†}	(Intercept)	1	518347.70	*
		Habitat-land-use	34	52210.80	*
		CC	1	26802.10	*
		LUC	2	13961.50	*
		LUC:Habitat-land-use	68	4160.20	*

	CC:LUC:Habitat-land-use	68	4124.60	*
	CC:LUC	2	3329.10	*
	CC:Habitat-land-use	34	3013.60	*
Trait α-diversity (FEve)				
FEve ~ (Habitat-land-use + CC + LUC)[3†]	(Intercept)	1	2852167.70	*
	LUC	2	22672.20	*
	CC	1	15177.60	*
	CC:LUC	2	10066.50	*
	Habitat-land-use	34	5504.80	*
	CC:Habitat-land-use	34	1249.60	*
	LUC:Habitat-land-use	68	1079.40	*
	CC:LUC:Habitat-land-use	68	588.60	*
Trait α-diversity (FDis)				
FDis ~ (Habitat-land-use + CC + LUC)[3†]	(Intercept)	1	19677794	*
	CC:LUC	2	86539	*
	Habitat-land-use	34	15511	*

		LUC	2	12258	*
		CC:Habitat-land-use	34	6257	*
		CC	1	5005	*
		LUC:Habitat-land-use	68	4541	*
		CC:LUC:Habitat-land-use	68	1757	*
	Trait α-diversity (FDiv)				
	FDiv ~ (Habitat-land-use + CC + LUC)^{3†}	(Intercept)	1	62536563	*
		LUC	2	63151	*
		CC	1	6930	*
		Habitat-land-use	34	6524	*
		CC:LUC	2	4040	*
		LUC:Habitat-land-use	68	2234	*
		CC:Habitat-land-use	34	613	*
		CC:LUC:Habitat-land-use	68	292	*
SET 2	**Trait α-diversity (FRic)**				
	FRic ~ (Habitat-land-use + CC)^{2†}	(Intercept)	1	251698.56	*

	Habitat-land-use	48	19933.83	*
	CC	1	7138.96	*
	CC:Habitat-land-use	48	3160.08	*
Trait α-diversity (FEve)				
FEve ~ (Habitat-land-use + CC)^{2†}	Habitat-land-use	48	2024.01	*
(ANOVA)	CC:Habitat-land-use	48	222.51	*
	CC	1	1.49	
	Residuals	9698		
Trait α-diversity (FDis)				
FDis ~ (Habitat-land-use + CC)^{2†}	CC	1	262057.00	*
(ANOVA)	Habitat-land-use	48	64531.00	*
	CC:Habitat-land-use	48	17040	*
	Residuals	9800		
Trait α-diversity (FDiv)				
FDiv ~ (Habitat-land-use + CC)^{2†}	(Intercept)	1	9080792	*
	Habitat-land-use	48	1198	*

		CC:Habitat-land-use	48	180	*
		CC	1	8	*
SET 1	**Productivity**				
	Productivity ~ (Habitat-land-use + CC + LUC)^{3}†	(Intercept)	1	1501126403	*
		Habitat-land-use	34	130709416	*
		LUC	2	54725448	*
		CC	1	8782855	*
		CC:Habitat-land-use	34	2608206	*
		LUC:Habitat-land-use	68	2170306	*
		CC:LUC	2	136463	*
		CC:LUC:Habitat-land-use	68	41973	*
SET 2	**Productivity**				
	Productivity ~ (Habitat-land-use + CC)^{2}†	(Intercept)	1	572526574	*
		Habitat-land-use	48	55372872	*
		CC	1	6101056	*
		CC:Habitat-land-use	48	1138545	*

[*]Significant at p-value < 0.01

[†]Superscripts “2” and “3” indicate the inclusion of all main factors, their two-way and three-way interactions (in case of “3”) in the model.

SUPPORTING INFORMATION – FIGURES

Figure S1 – Maps of a) current habitat types and b) current and potential land-use regimes in the Ecrins National Park and c) elevation in meters a.s.l. Habitats were classified following the DELPHINE habitat classification of the park (Esterni *et al.* 2006) and land-use regimes followed (Boulangeat *et al.* 2014a). Presently grazed areas (with intensities ‘low’, ‘medium’ and ‘high’ numbered sequentially) and mown areas are shown in the top-left and top-right panels of figure b), respectively. Future grazed areas (grazed at the highest grazing intensity) and future mown areas are shown in the bottom-left and bottom-right panels, respectively. Non-disturbed areas correspond to all areas that are not currently grazed or mown (light green); future non-disturbed areas are areas that will not be grazed or mown under land-use intensification scenarios (dark green).

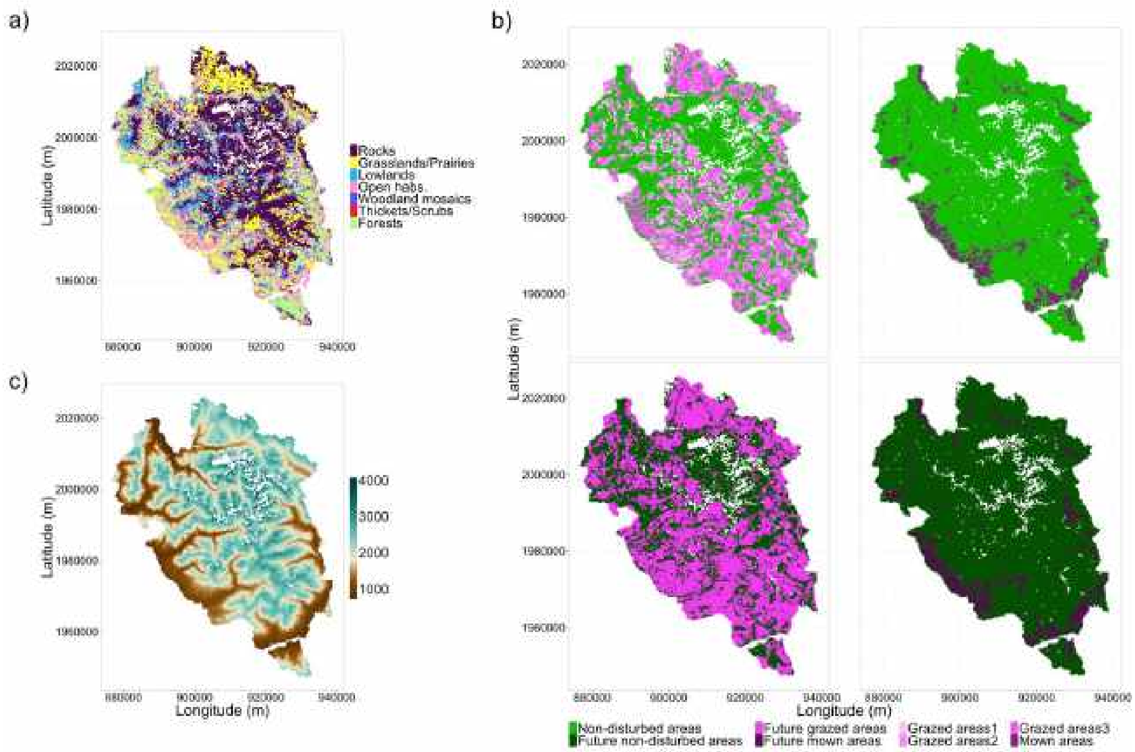

Figure S2 – Overall cumulative curve of the proportion of variance explained by principal components (PCs). The mean cumulative of explained variance is shown in function of dimensionality, across all Principal Components Analyses (PCAs) calculated on raw plant functional groups' (PFG) abundances. Cumulative explained variances were averaged at each number of PCs across scenario and habitat-land-use combinations. The inflexion point of the curve was taken to be at the 6th PC (shown as the vertical dashed line), which meant that building hypervolumes using 6 PCs explained over 95% of the total variance.

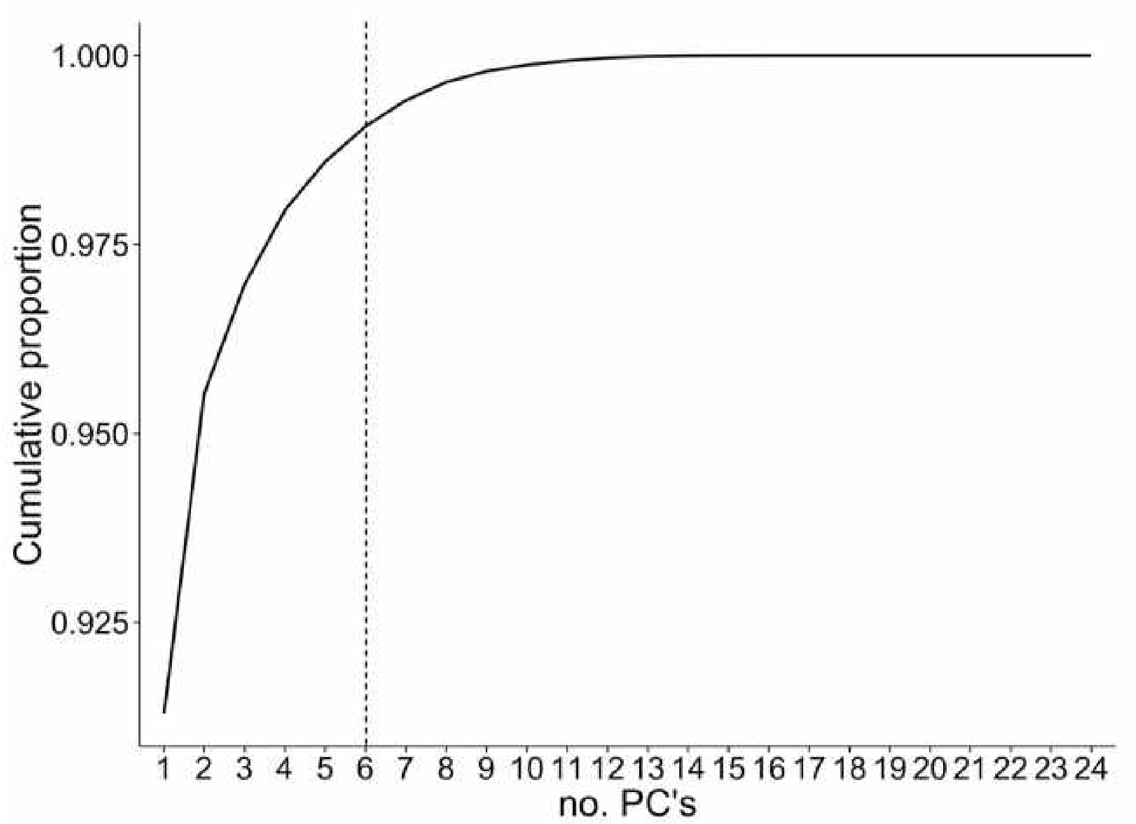

Figure S3 – Fitted proportion of overlap by scenario and habitat-land-use combination. Fitted values of proportion of overlap (overlap) between control and post-perturbation hypervolumes built are shown for a) raw PFG abundances and b) CWM trait values. Fitted values were calculated from the best models relating the square-root proportion of overlap with climate change, land-use changes, habitat-land-use combinations and their interactions (see Table S2) and are shown by habitat-land-use combination in each scenario, after being back-transformed. Standard errors of the observed means and of fitted values are shown as error bars. Grazing intensities low, medium and high are coded 'grazed areas1', 'grazed areas2' and 'grazed areas3', respectively. Comparisons between proof-of-concept ('POC') and control scenario hypervolumes are also included.

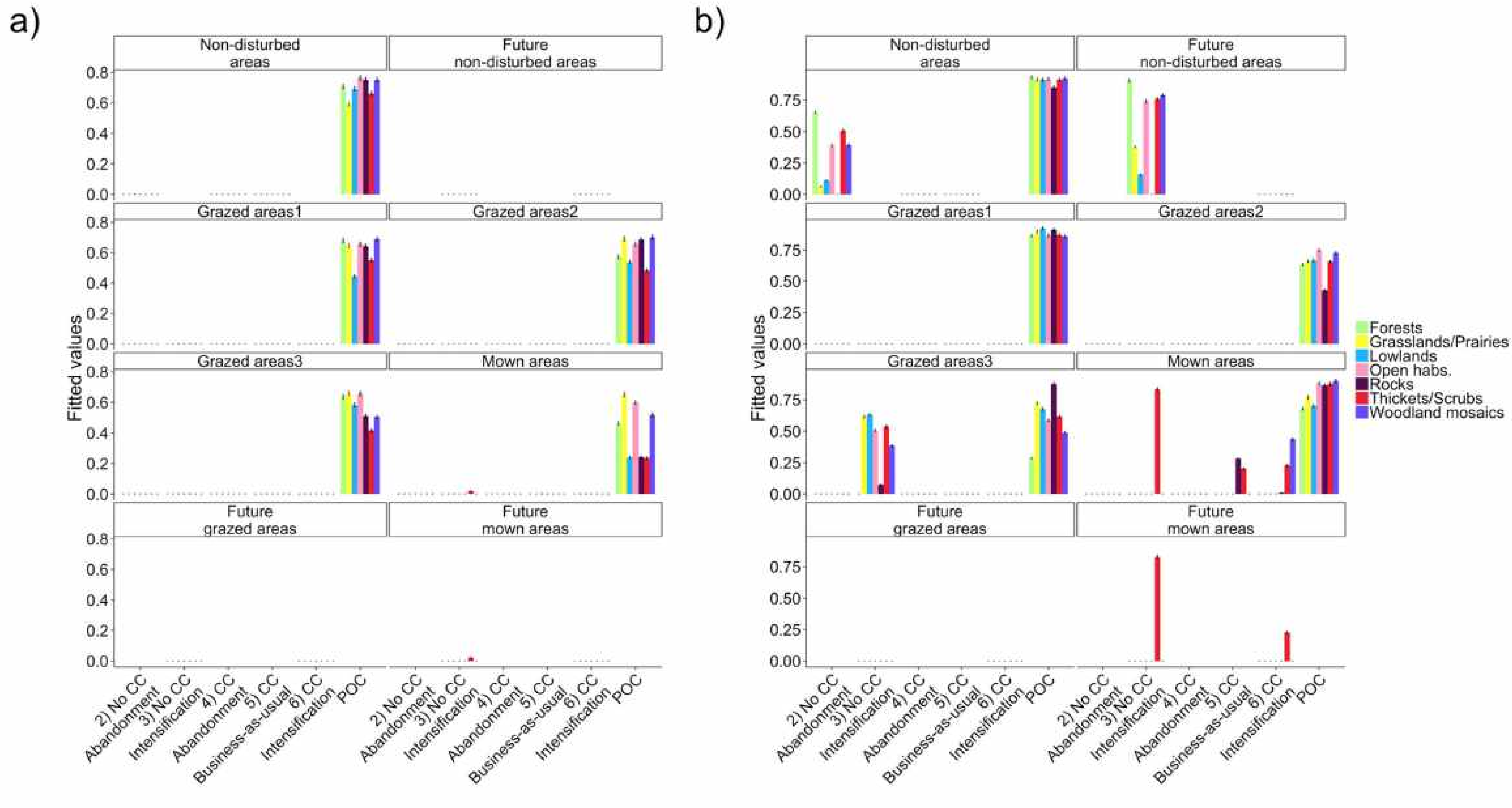

a)
b)
Non-disturbed areas
Future non-disturbed areas
Grazed areas1
Grazed areas2
Grazed areas3
Mown areas
Future grazed areas
Future mown areas
Fitted values
0.0
0.2
0.4
0.6
0.8
0.00
0.25
0.50
0.75
2) No CC Abandonment
3) No CC Intensification
4) CC Abandonment
5) CC Business-as-usual
6) CC Intensification
POC
Forests
Grasslands/Prairies
Lowlands
Open habs.
Rocks
Thickets/Scrubs
Woodland mosaics

Figure S4 – Relationship between hypervolume size and the proportion of overlap. Relationships between the proportion of overlap (overlap) between control and post-perturbation hypervolumes ('HV') and their sizes are shown for each scenario, for a) hypervolumes based on raw PFG abundances and on b) community weighted mean (CWM) trait values. Proof-of concept ('POC') comparisons for each set of components are also shown. Overlap values were square-rooted to follow linear model assumptions and improve model fit. Each point represents a habitat-land-use combination for a given repetition (sample size varying between 105 and 147 depending on scenarios). Information on adjusted R^2 and coefficient values (next to each line) is shown for significant relationships only. Shaded areas denote confidence intervals at 95%.

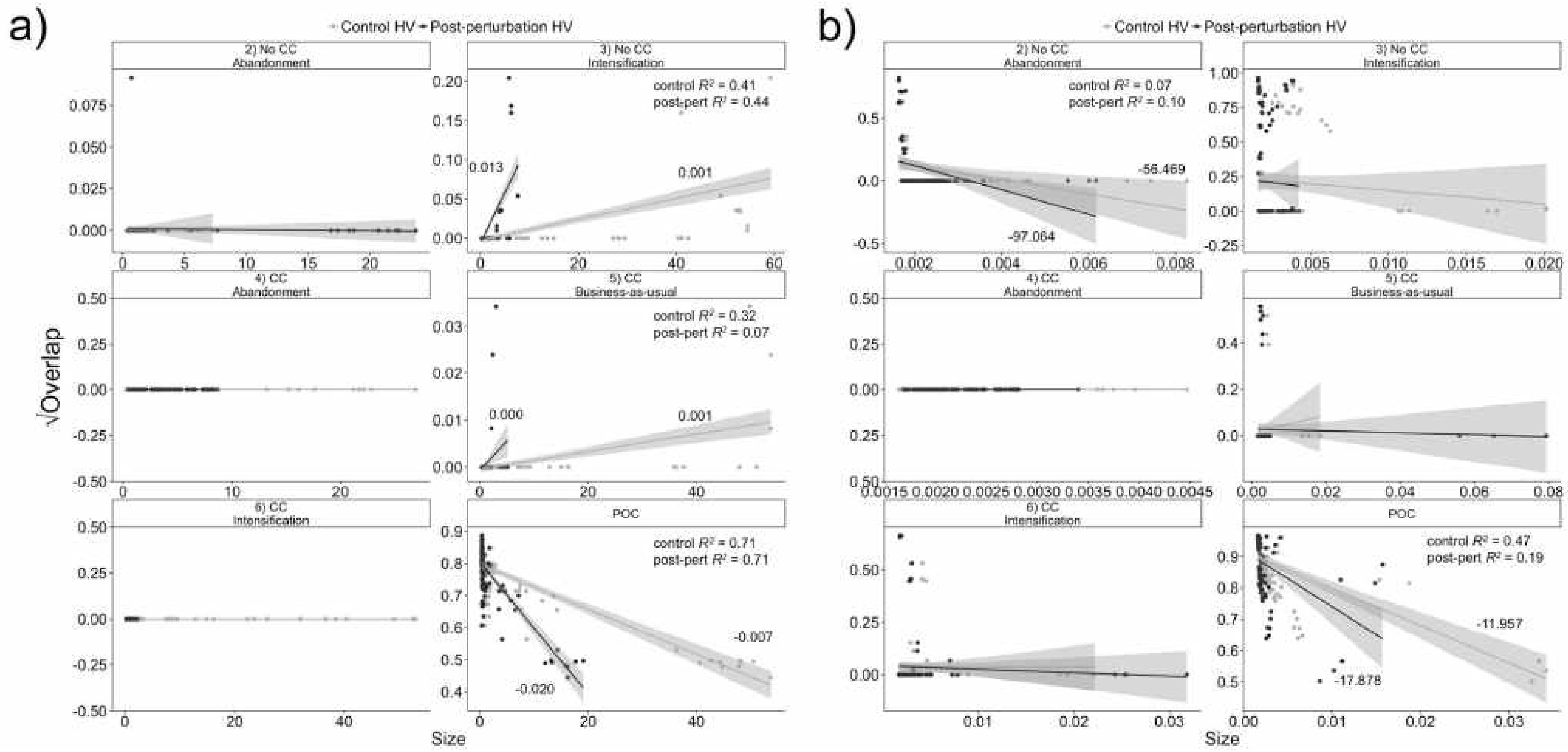

a)
Control HV
Post-perturbation HV
2) No CC Abandonment
3) No CC Intensification
control R^2 = 0.41
post-pert R^2 = 0.44
0.013
0.001
4) CC Abandonment
5) CC Business-as-usual
control R^2 = 0.32
post-pert R^2 = 0.07
0.000
0.001
6) CC Intensification
POC
control R^2 = 0.71
post-pert R^2 = 0.71
-0.007
-0.020
√Overlap
Size
b)
Control HV
Post-perturbation HV
2) No CC Abandonment
control R^2 = 0.07
post-pert R^2 = 0.10
-56.469
-97.064
3) No CC Intensification
4) CC Abandonment
5) CC Business-as-usual
6) CC Intensification
POC
control R^2 = 0.47
post-pert R^2 = 0.19
-11.957
-17.878
Size

Figure S5 – Fitted hypervolume centroid distances by scenario and habitat-land-use combination. Fitted distances between control and post-perturbation hypervolume centroids built are shown for a) raw PFG abundances and b) CWM trait values. Fitted values were calculated from the best models relating the centroid distances with climate change, land-use changes, habitat-land-use combinations and their interactions (see Table S2) and are shown by habitat-land-use combination in each scenario. Standard errors of the observed means and of fitted values are shown as error bars. Grazing intensities low, medium and high are coded 'grazed areas1', 'grazed areas2' and 'grazed areas3', respectively. Comparisons between proof-of-concept ('POC') and control scenario hypervolumes are also included.

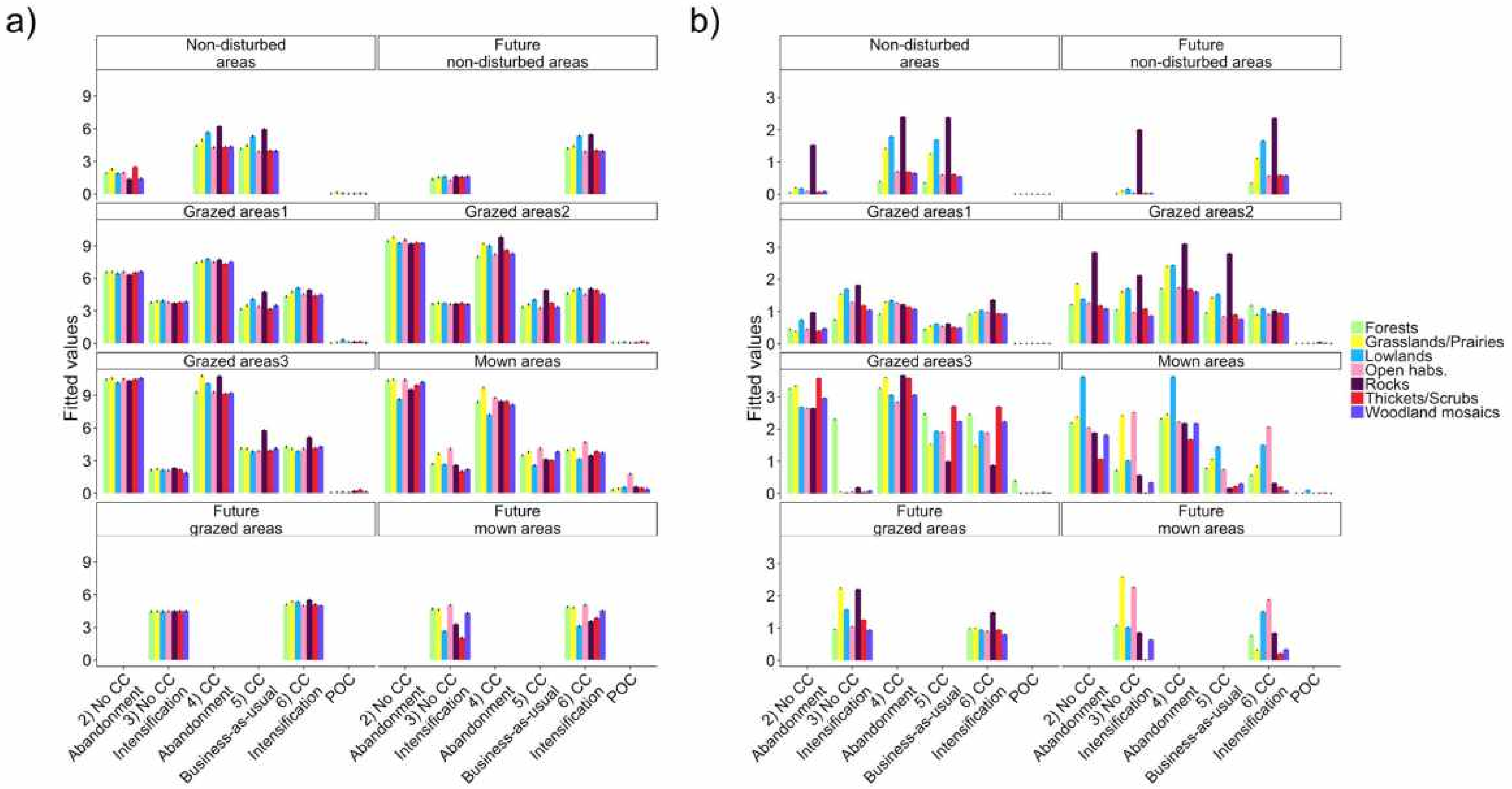
a)
b)
Non-disturbed areas
Future non-disturbed areas
Grazed areas1
Grazed areas2
Grazed areas3
Mown areas
Future grazed areas
Future mown areas
Fitted values
2) No CC Abandonment
3) No CC Intensification
4) CC Abandonment
5) CC Business-as-usual
6) CC Intensification
POC
Forests
Grasslands/Prairies
Lowlands
Open habs.
Rocks
Thickets/Scrubs
Woodland mosaics

Figure S6 – Fitted hypervolume size changes by scenario and habitat-land-use combination. Hypervolume size changes (Δsize) were calculated as the difference between post-perturbation and control hypervolumes (negative values indicating size reductions and positive values indicating size increases). Fitted size changes are shown for hypervolumes built from a) raw PFG abundances and b) CWM trait values. Fitted values were calculated from the best models relating the centroid distances with climate change, land-use changes, habitat-land-use combinations and their interactions (see Table S2) and are shown by habitat-land-use combination in each scenario. Standard errors of the observed means and of fitted values are shown as error bars. Grazing intensities low, medium and high are coded 'grazed areas1', 'grazed areas2' and 'grazed areas3', respectively. Comparisons between proof-of-concept ('POC') and control scenario hypervolumes are also included.

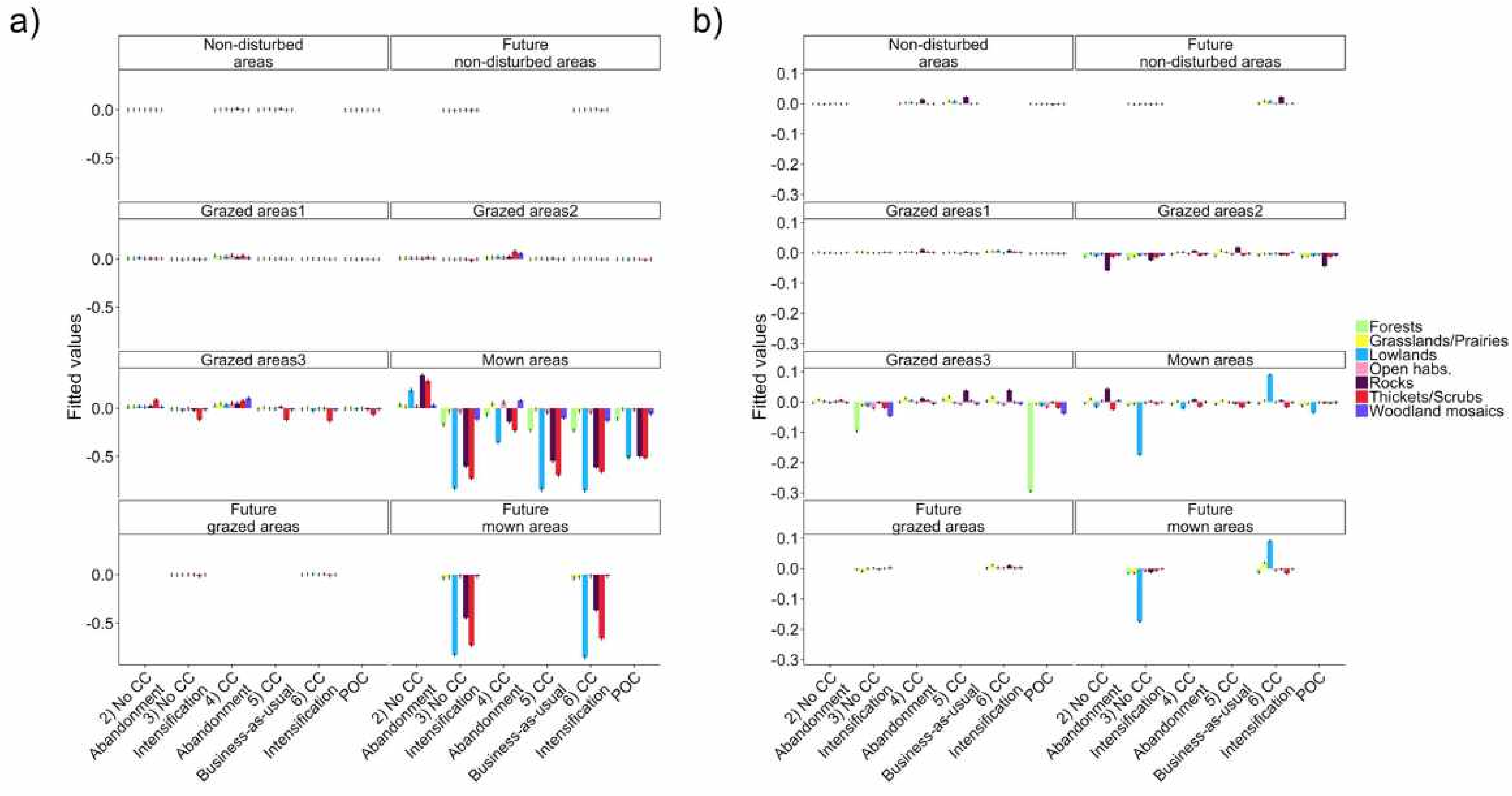

a)
b)
Non-disturbed areas
Future non-disturbed areas
Grazed areas1
Grazed areas2
Grazed areas3
Mown areas
Future grazed areas
Future mown areas
Fitted values
Forests
Grasslands/Prairies
Lowlands
Open habs.
Rocks
Thickets/Scrubs
Woodland mosaics
2) No CC Abandonment
3) No CC Intensification
4) CC Abandonment
5) CC Business-as-usual
6) CC Intensification
POC

1

2

Figure S7 – Taxonomic diversity by scenario and habitat-land-use combination. Taxonomic diversity was calculated yearly as the inverse Simpson concentration (Leinster & Cobbold 2012), based on PFG abundances of the last 100 years of the control and scenario simulations. Calculations were done per scenario and habitat-land-use combination and averaged across repetitions. Fitted values were calculated from the best models explaining the variation of PFG diversity in function of climate change, land-use changes and habitat-land-use combinations. To guarantee a balanced design, models were broken in two sets. The first set investigating the effects of CC and LUC on "current" habitat-land-use combinations ('set 1' shown in panel a)) and the second to investigate the effects of CC and all habitat-land-use combinations on scenarios of LU intensification ('set 2', shown in panel b); see Table S3). Grazing intensities low, medium and high are coded 'grazed areas1', 'grazed areas2' and 'grazed areas3', respectively.

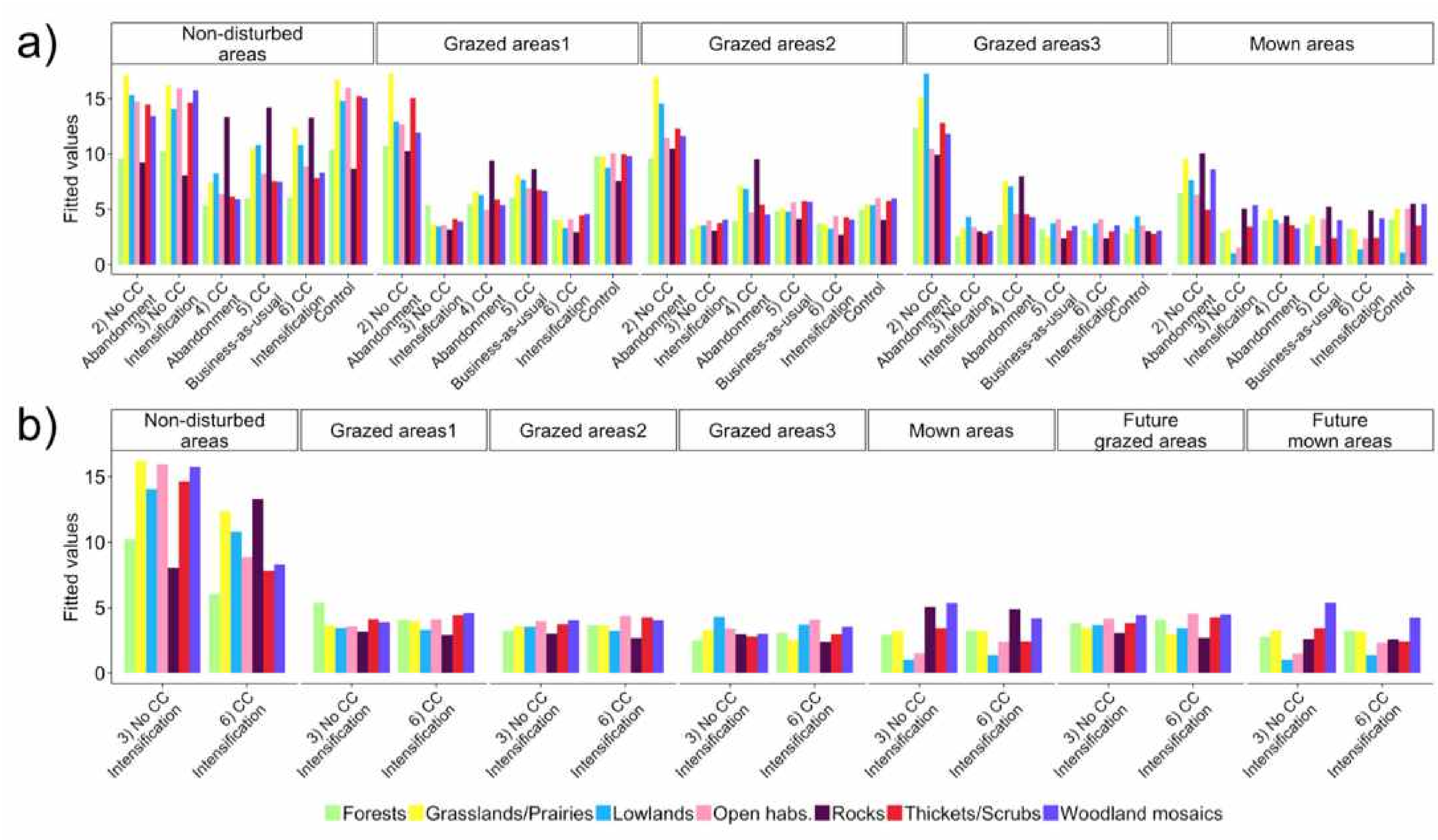
a)
Non-disturbed areas
Grazed areas1
Grazed areas2
Grazed areas3
Mown areas
Fitted values
2) No CC Abandonment
3) No CC Intensification
4) CC Abandonment
5) CC Business-as-usual
6) CC Intensification
Control
b)
Non-disturbed areas
Grazed areas1
Grazed areas2
Grazed areas3
Mown areas
Future grazed areas
Future mown areas
Fitted values
3) No CC Intensification
6) CC Intensification
Forests
Grasslands/Prairies
Lowlands
Open habs.
Rocks
Thickets/Scrubs
Woodland mosaics

Figure S8 – Functional diversity by scenario and habitat-land-use combination, first set of models. Functional diversity was estimated using four functional diversity indices: functional richness (FRic), functional evenness (FEve), functional divergence (FDiv; Villéger *et al.* 2008) and functional dispersion (FDis; Laliberté & Legendre 2010), calculated for the traits used to build trait hypervolumes (specific leaf area, log height, log seed mass and palatability). All indices were calculated yearly for the last 100 years of the control and scenario simulations. Fitted values shown in the figure were calculated from the best models explaining the variation of functional diversity indices in function of climate change, land-use changes and habitat-land-use combinations. Details on statistical analyses and a presentation of results obtained for FRic and FDiv are available in Appendix S2. Only the first set of models ('set 1'; see Table S3) is shown here for a) FRic, b) FEve, c) FDis and d) FDiv. The first set of models investigates the effects of CC and LUC on "current" habitat-land-use combinations. Grazing intensities low, medium and high are coded 'grazed areas1', 'grazed areas2' and 'grazed areas3', respectively.

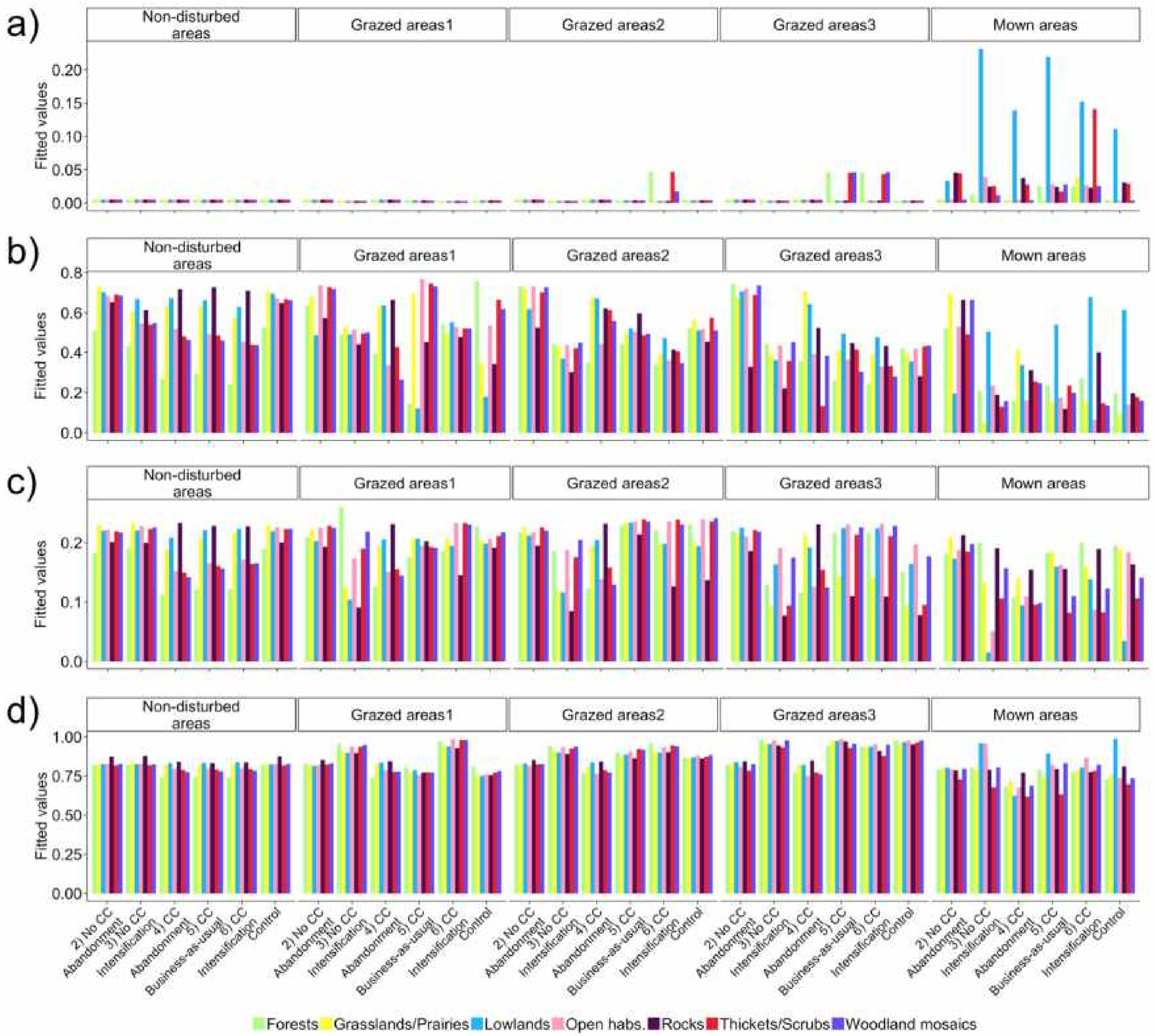
a)
b)
c)
d)
Non-disturbed areas
Grazed areas1
Grazed areas2
Grazed areas3
Mown areas
Fitted values
2) No CC Abandonment
3) No CC Intensification
4) CC Abandonment
5) CC Business-as-usual
6) CC Intensification
Control
Forests
Grasslands/Prairies
Lowlands
Open habs.
Rocks
Thickets/Scrubs
Woodland mosaics

1

Figure S9 – Functional diversity by scenario and habitat-land-use combination, second set of models. Functional diversity was estimated using four functional diversity indices: functional richness (FRic), functional evenness (FEve), functional divergence (FDiv; Villéger *et al.* 2008) and functional dispersion (FDis; Laliberté & Legendre 2010), calculated for the traits used to build trait hypervolumes (specific leaf area, log height, log seed mass and palatability). All indices were calculated yearly for the last 100 years of the control and scenario simulations. Fitted values shown in the figure were calculated from the best models explaining the variation of functional diversity indices in function of climate change, land-use changes and habitat-land-use combinations. Details on statistical analyses and a presentation of results obtained for FRic and FDiv are available in Appendix S2. The second set of models ('set 2'; see Table S3) is shown here for a) FRic, b) FEve, c) FDis and d) FDiv. This set of models investigates the effects of CC and all habitat-land-use combinations on scenarios of LU intensification. Grazing intensities low, medium and high are coded 'grazed areas1', 'grazed areas2' and 'grazed areas3', respectively.

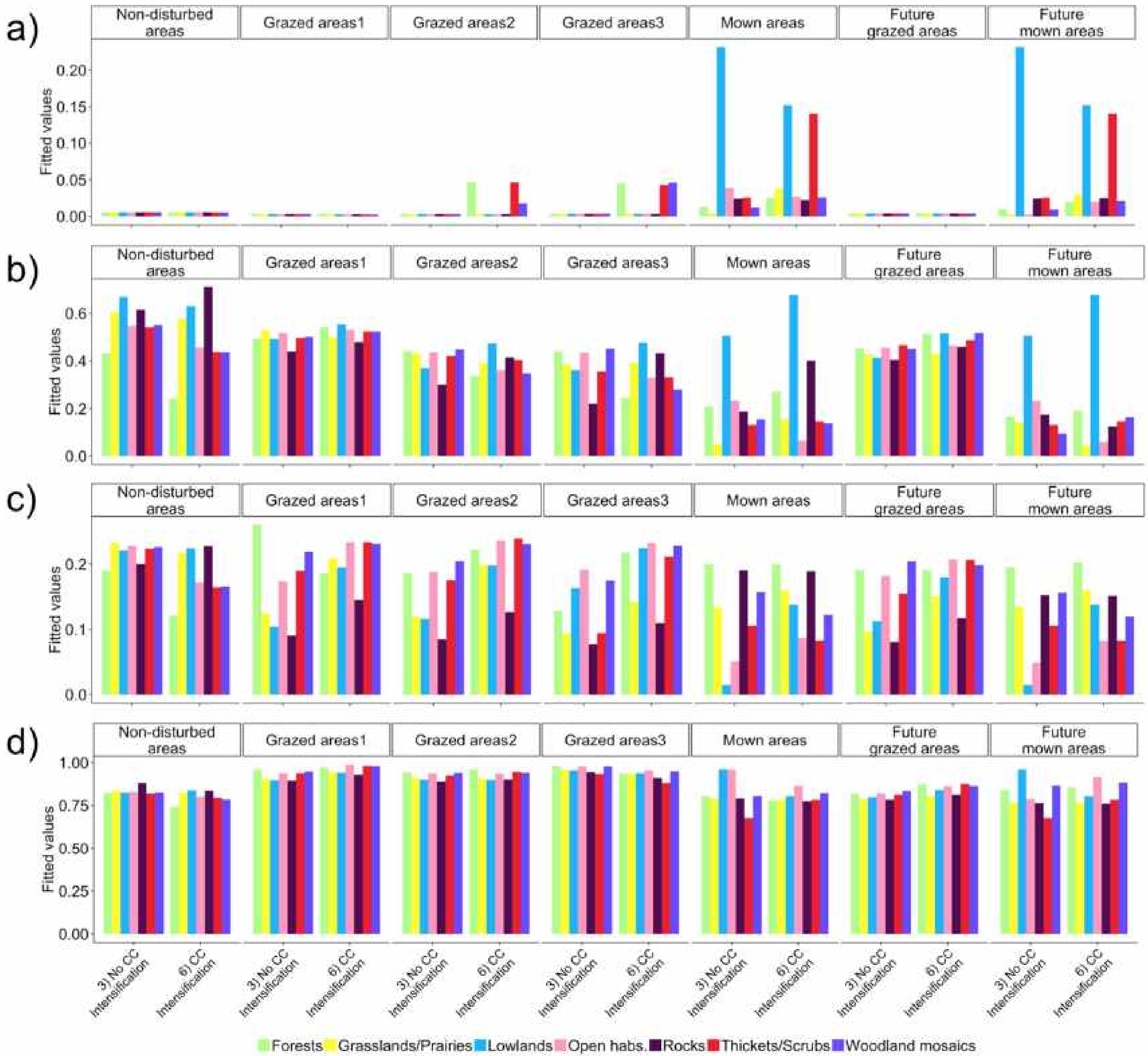

a)
b)
c)
d)
Non-disturbed areas
Grazed areas1
Grazed areas2
Grazed areas3
Mown areas
Future grazed areas
Future mown areas
Fitted values
3) No CC Intensification
6) CC Intensification
Forests
Grasslands/Prairies
Lowlands
Open habs.
Rocks
Thickets/Scrubs
Woodland mosaics

61

Figure S10 – Productivity by scenario and habitat-land-use combination. Productivity was calculated yearly as the sum of PFG raw abundances, for the last 100 years of the control and scenario simulations. Fitted values were calculated from the best models explaining the variation of productivity in function of climate change, land-use changes and habitat-land-use combinations. To guarantee a balanced design, models were broken in two sets. The first set investigating the effects of CC and LUC on "current" habitat-land-use combinations ('set 1' shown in panel a)) and the second to investigate the effects of CC and all habitat-land-use combinations on scenarios of LU intensification ('set 2', shown in panel b); see Table S3). Grazing intensities low, medium and high are coded 'grazed areas1', 'grazed areas2' and 'grazed areas3', respectively.

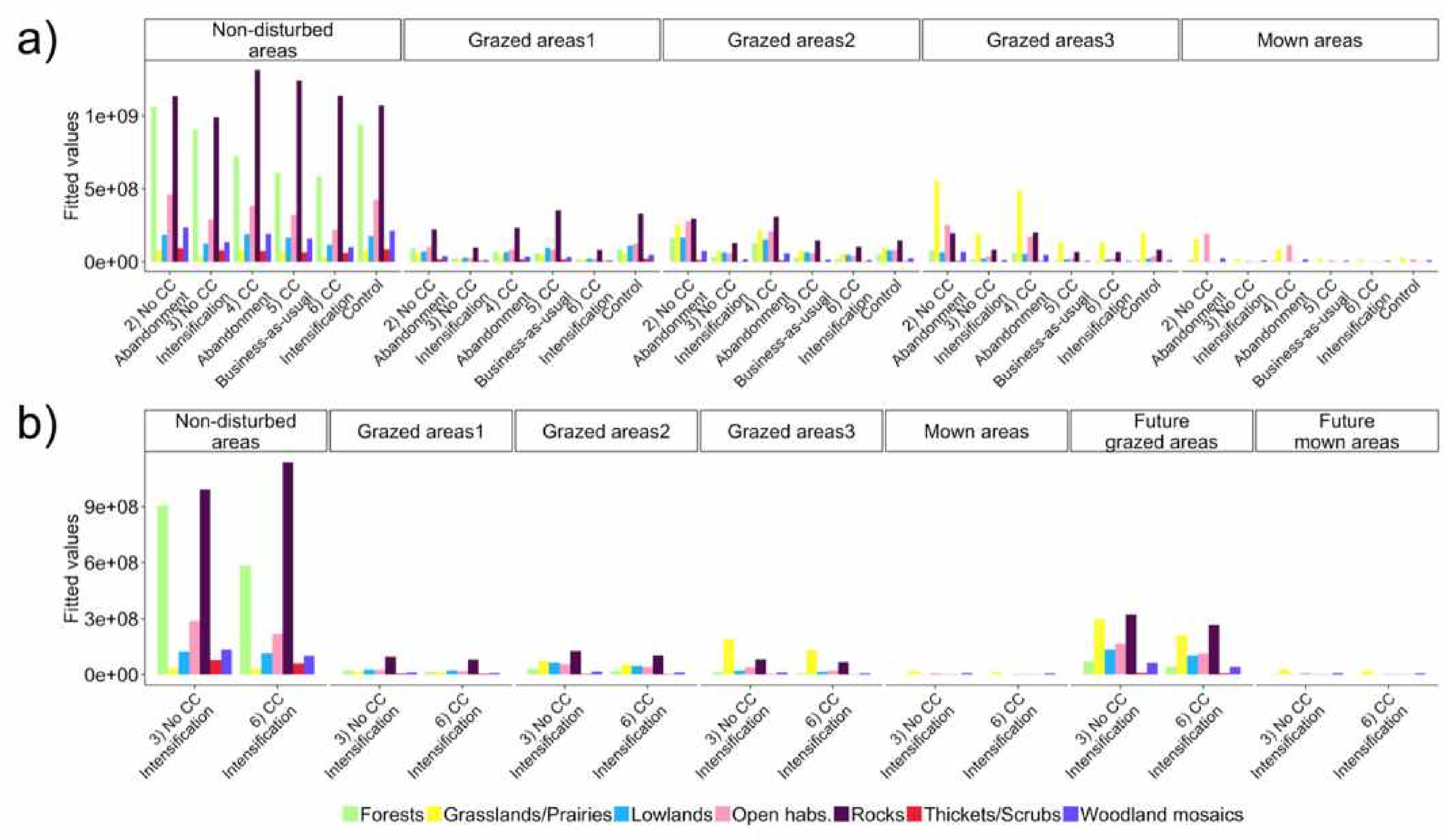
a)
Non-disturbed areas
Grazed areas1
Grazed areas2
Grazed areas3
Mown areas
Fitted values
1e+09
5e+08
0e+00
2) No CC Abandonment
3) No CC Intensification
4) CC Abandonment
5) CC Business-as-usual
6) CC Intensification
Control
b)
Non-disturbed areas
Grazed areas1
Grazed areas2
Grazed areas3
Mown areas
Future grazed areas
Future mown areas
Fitted values
9e+08
6e+08
3e+08
0e+00
3) No CC Intensification
6) CC Intensification
Forests
Grasslands/Prairies
Lowlands
Open habs.
Rocks
Thickets/Scrubs
Woodland mosaics

References

Asner G.P., Elmore A.J., Olander L.P., Martin R.E. & Harris A.T. (2004). Grazing systems, ecosystem responses, and global change. *Annual Review of Environment and Resources*, 29, 261-299.

Beisner B.E., Haydon D.T. & Cuddington K. (2003). Alternative stable states in ecology. *Frontiers in Ecology and the Environment*, 1, 376-382.

Blonder B., Lamanna C., Violle C. & Enquist B.J. (2014). The n‐dimensional hypervolume. *Global Ecology and Biogeography*, 23, 595-609.

Boulangeat I., Georges D., Dentant C., Bonet R., Van Es J., Abdulhak S., Zimmermann N.E. & Thuiller W. (2014a). Anticipating the spatio-temporal response of plant diversity and vegetation structure to climate and land use change in a protected area. *Ecography*, 37, 1230-1239.

Boulangeat I., Georges D. & Thuiller W. (2014b). FATE‐HD: a spatially and temporally explicit integrated model for predicting vegetation structure and diversity at regional scale. *Global Change Biology*, 20, 2368-2378.

Boulangeat I., Philippe P., Abdulhak S., Douzet R., Garraud L., Lavergne S., Lavorel S., Van Es J., Vittoz P. & Thuiller W. (2012). Improving plant functional groups for dynamic models of biodiversity: at the crossroads between functional and community ecology. *Global Change Biology*, 18, 3464-3475.

Cadotte M.W., Dinnage R. & Tilman D. (2012). Phylogenetic diversity promotes ecosystem stability. *Ecology*, 93, S223-S233.

Dakos V., Carpenter S.R., Brock W.A., Ellison A.M., Guttal V., Ives A.R., Kéfi S., Livina V., Seekell D.A., van Nes E.H. & Scheffer M. (2012). Methods for detecting early warnings of critical transitions in time series illustrated using simulated ecological data. *PLoS ONE*, 7, e41010.

Dakos V., Carpenter S.R., van Nes E.H. & Scheffer M. (2015). Resilience indicators: prospects and limitations for early warnings of regime shifts. *Philosophical Transactions of the Royal Society of London B: Biological Sciences*, 370, 20130263.

de Bello F., Lavorel S., Lavergne S., Albert C.H., Boulangeat I., Mazel F. & Thuiller W. (2013). Hierarchical effects of environmental filters on the functional structure of plant communities: a case study in the French Alps. *Ecography*, 36, 393-402.

Esterni M., Rovera G., Bonet R., Salomez P., Cortot H. & Guilloux J. (2006). DELPHINE - Découpage de l'Espace en Liaison avec les Potentialités Humaines et en Interrelation avec la Nature. In. Parc National des Ecrins.

Gottfried M., Pauli H., Futschik A., Akhalkatsi M., Barančok P., Alonso J.L.B., Coldea G., Dick J., Erschbamer B. & Kazakis G. (2012). Continent-wide response of mountain vegetation to climate change. *Nature Climate Change*, 2, 111-115.

Gunderson L.H. (2000). Ecological resilience - in theory and application. *Annual Review of Ecology and Systematics*, 35, 425-439.

Holling C.S. (1996). Engineering resilience vs. ecological resilience. In: *Engineering Within Ecological Constraints* (ed. Schulze PC). National Academy Press Washington, D.C., pp. 31-43.

Horan R.D., Fenichel E.P., Drury K.L. & Lodge D.M. (2011). Managing ecological thresholds in coupled environmental–human systems. *Proceedings of the National Academy of Sciences*, 108, 7333-7338.

Kattge J., Díaz S., Lavorel S., Prentice I.C., Leadley P., Bönisch G., Garnier E., Westoby M., Reich P.B., Wright I.J., Cornelissen J.H.C., Violle C., Harrison S.P., Bodegom P.M.v., Reichstein M., Enquist B.J., Soudzilovskaia N.A., Ackerly D.D., Anand M., Atkin O., Bahn M., Baker T.R., Baldocchi D., Bekker R., Blanco C., Blonder B., Bond W.J., Bradstock R., Bunker D.E., Casanoves F., Cavender-Bares J., Chambers J.Q., Chapin

F.S., Chave J., Coomes D., Cornwell W.K., Craine J.M., Dobrin B.H., Duarte L., Durka W., Elser J., Esser G., Estiarte M., Fagan W.F., Fang J., Fernández-Méndez F., Fidelis A., Finegan B., Flores O., Ford H., Frank D., Freschet G.T., Fyllas N.M., Gallagher R.V., Green W.A., Gutierrez A.G., Hickler T., Higgins S., Hodgson J.G., Jalili A., Jansen S., Joly C., Kerkhoff A.J., Kirkup D., Kitajima K., Kleyer M., Klotz S., Knops J.M.H., Kramer K., Kühn I., Kurokawa H., Laughlin D., Lee T.D., Leishman M., Lens F., Lenz T., Lewis S.L., Lloyd J., Llusià J., Louault F., Ma S., Mahecha M.D., Manning P., Massad T., Medlyn B., Messier J., Moles A.T., Müller S.C., Nadrowski K., Naeem S., Niinemets Ü., Nöllert S., Nüske A., Ogaya R., Oleksyn J., Onipchenko V.G., Onoda Y., Ordoñez J., Overbeck G., Ozinga W.A., Patiño S., Paula S., Pausas J.G., Peñuelas J., Phillips O.L., Pillar V., Poorter H., Poorter L., Poschlod P., Prinzing A., Proulx R., Rammig A., Reinsch S., Reu B., Sack L., Salgado-Negret B., Sardans J., Shiodera S., Shipley B., Siefert A., Sosinski E., Soussana J.-F., Swaine E., Swenson N., Thompson K., Thornton P., Waldram M., Weiher E., White M., White S., Wright S.J., Yguel B., Zaehle S., Zanne A.E. & Wirth C. (2011). TRY - a global database of plant traits. *Global Change Biology*, 17, 2905-2935.

Laliberté E. & Legendre P. (2010). A distance-based framework for measuring functional diversity from multiple traits. *Ecology*, 91, 299-305.

Leinster T. & Cobbold C.A. (2012). Measuring diversity: the importance of species similarity. *Ecology*, 93, 477-489.

Mori A.S., Furukawa T. & Sasaki T. (2013). Response diversity determines the resilience of ecosystems to environmental change. *Biological Reviews*, 88, 349-364.

Mouillot D., Graham N.A.J., Villéger S., Mason N.W.H. & Bellwood D.R. (2013). A functional approach reveals community responses to disturbances. *Trends in Ecology and Evolution*, 28, 167-177.

Norberg J. (2004). Biodiversity and ecosystem functioning: a complex adaptive systems approach. *Limnology and Oceanography*, 49, 1269-177.

Pauli H., Gottfried M., Reiter K., Klettner C. & Grabherr G. (2007). Signals of range expansions and contractions of vascular plants in the high Alps: observations (1994–2004) at the GLORIA* master site Schrankogel, Tyrol, Austria. *Global Change Biology*, 13, 147-156.

Pavoine S. & Bonsall M.B. (2009). Biological diversity: distinct distributions can lead to the maximization of Rao's quadratic entropy. *Theoretical population biology*, 75, 153-163.

Pavoine S. & Bonsall M.B. (2011). Measuring biodiversity to explain community assembly: a unified approach. *Biological Reviews*, 86, 792-812.

Scheffer M., Bascompte J., Brock W.A., Brovkin V., Carpenter S.R., Dakos V., Held H., van Nes E.H., Rietkerk M. & Sugihara G. (2009). Early-warning signals for critical transitions. *Nature*, 461, 53-59.

Sharma Y., Abbott K.C., Dutta P.S. & Gupta A. (2015). Stochasticity and bistability in insect outbreak dynamics. *Theoretical Ecology*, 8, 163-174.

Tasser E. & Tappeiner U. (2002). Impact of land use changes on mountain vegetation. *Applied vegetation science*, 5, 173-184.

Thuiller W., Lafourcade B., Engler R. & Araújo M.B. (2009). BIOMOD–a platform for ensemble forecasting of species distributions. *Ecography*, 32, 369-373.

Tucker C.M., Cadotte M.W., Carvalho S.B., Davies T.J., Ferrier S., Fritz S.A., Grenyer R., Helmus M.R., Jin L.S. & Mooers A.O. (2016). A guide to phylogenetic metrics for conservation, community ecology and macroecology. *Biological reviews of the Cambridge Philosophical Society*.

Villéger S., Mason N.W. & Mouillot D. (2008). New multidimensional functional diversity indices for a multifaceted framework in functional ecology. *Ecology*, 89, 2290-2301.

Westoby M. (1998). A leaf-height-seed (LHS) plant ecology strategy scheme. *Plant and Soil*, 199, 213-227.